

# Renormalon-based resummation of Bjorken polarised sum rule in perturbative and holomorphic QCD

César Ayala<sup>a,\*</sup>, Camilo Castro-Arriaza<sup>b,†</sup> and Gorazd Cvetič<sup>b,‡</sup>

<sup>a</sup>*Instituto de Alta Investigación, Sede La Tirana,*

*Universidad de Tarapacá, Av. La Tirana 4802, Iquique, Chile and*

<sup>b</sup>*Department of Physics, Universidad Técnica Federico Santa María, Avenida España 1680, Valparaíso, Chile*

(Dated: January 25, 2024)

The present knowledge of the renormalon structure of Bjorken polarised sum rule (BSR)  $\bar{\Gamma}_1^{p-n}(Q^2)$  is used to construct its characteristic function and thus to evaluate the leading-twist part of BSR. In this resummation, we take for the running coupling either the perturbative QCD (pQCD) coupling  $a(Q^2) \equiv \alpha_s(Q^2)/\pi$  in specific schemes, or holomorphic couplings  $[(a(Q^2) \mapsto \mathcal{A}(Q^2))]$  that have no Landau singularities. The  $D = 2$  and  $D = 4$  terms are included in the Operator Product Expansion (OPE) of inelastic BSR, and fits are performed to the available experimental data in various intervals  $(Q_{\min}^2, Q_{\max}^2)$  where  $Q_{\max}^2 = 4.74 \text{ GeV}^2$ . Since the pQCD coupling  $a(Q^2)$  has Landau singularities at  $Q^2 \lesssim 1 \text{ GeV}^2$ , we need relatively high  $Q_{\min}^2 \approx 1.7 \text{ GeV}^2$  in the pQCD case. When holomorphic couplings  $\mathcal{A}(Q^2)$  are used, no such problems occur; for the  $3\delta\text{AQCD}$  and  $2\delta\text{AQCD}$  variants the preferred values are  $Q_{\min}^2 \approx 0.6 \text{ GeV}^2$ . The preferred values of  $\alpha_s$  in general cannot be unambiguously extracted, due to large uncertainties of the experimental BSR data, although the fit with  $2\delta\text{AQCD}$  and the  $D = 2$  term included suggests  $\alpha_s^{\overline{\text{MS}}}(M_Z^2) \approx 0.1181$ . At fixed value of  $\alpha_s^{\overline{\text{MS}}}(M_Z^2)$ , the values of the  $D = 2$  and  $D = 4$  residue parameters are determined in all cases, with the corresponding uncertainties.

Keywords: renormalons; resummations; perturbative QCD; holomorphic QCD; QCD phenomenology

## I. INTRODUCTION

We analyse in this work the inelastic polarised Bjorken sum rule (BSR)  $\bar{\Gamma}_1^{p-n}(Q^2)$  [1, 2], which is the difference of the spin-dependent structure functions of proton and neutron integrated over the  $x$ -Bjorken parameter range  $0 < x < 1$ . Its Operator Product Expansion (OPE) has a relatively simple form, because it is an isovector and spacelike quantity.

Experimental results for  $\bar{\Gamma}_1^{p-n}(Q^2)$ , though often with significant statistical and systematic uncertainties, are available from various experiments: CERN [3], DESY [4], SLAC [5], and from various experiments at the Jefferson Lab [6–10]. These experimental results are based on the measured values of the spin-dependent structure functions over various values of Bjorken  $x$ , and over various values of  $Q^2$  in the wide range  $0.02 \text{ GeV}^2 < Q^2 < 5 \text{ GeV}^2$  where  $q^2 \equiv -Q^2$  is the squared momentum transfer.

On the other hand, the considered inelastic BSR  $\bar{\Gamma}_1^{p-n}(Q^2)$  is evaluated theoretically by using OPE that is usually truncated at the dimension  $D = 2$  ( $\sim 1/Q^2$ ) or  $D = 4$  ( $\sim 1/(Q^2)^2$ ) term. The leading-twist ( $D = 0$ ) term has the canonical QCD part  $d(Q^2)$  which is in general evaluated as a truncated perturbation series (TPS) in powers of the pQCD coupling  $a(Q^2) = \alpha_s(Q^2)/\pi$ . The values of the first four expansion coefficients (i.e., up to  $\sim a^4$ ) have been calculated exactly [11–13], and the value of the coefficient at  $a^5$  can be estimated. In this way, the mentioned OPE expression is then fitted to the experimental data, and the values of the OPE coefficient of the  $D = 2$  term, and possibly of the  $D = 4$  term, can be extracted. This pQCD OPE approach, or specific variants of it, has been followed in the works [6, 7, 9, 14–17].

The described approaches of theoretical evaluation do not involve direct resummations in the canonical QCD part of BSR,  $d(Q^2)$ . Analyses of BSR were also performed in the approaches that use holomorphic QCD running couplings  $a(Q^2) \mapsto \mathcal{A}(Q^2)$  (i.e., free of Landau singularities) in  $d(Q^2)$ , enabling the evaluation of  $d(Q^2)$  even at lower  $Q^2 \lesssim 1 \text{ GeV}^2$  [15]. However, even in those cases, the series for  $d(Q^2)$  were truncated. Actually, we know that  $d(Q^2)$  of BSR has the expansion coefficients  $d_n$  (at  $a^{n+1}$ ) that grow very fast with increasing  $n$ , approximately as  $d_n \sim n!(\beta_0/p)^n$  with  $p = 1$  (due to the leading infrared renormalon close to the origin,  $u = p = 1$ ), which indicates that truncation of  $d(Q^2)$ , at  $\sim a^4$  or  $\sim a^5$ , may miss important contributions.

\*Electronic address: c.ayala86@gmail.com

†Electronic address: camilo.castroa@sansano.usm.cl

‡Electronic address: gorazd.cvetic@gmail.com

<sup>1</sup> In [16, 17] the resummations are indirect, by fixing (various) renormalisation scale(s) in the TPS according to different criteria.

In this work we evaluate the QCD canonical part  $d(Q^2)$  of BSR by performing a renormalon-based resummation. The extension of the  $d(Q^2)$  expansion to higher powers of  $a$  is performed by a renormalon-based approach. The latter approach allows us to construct a characteristic function of  $d(Q^2)$  and enables us to perform resummation in a form of integration that involves  $a(\mu^2)$  over the entire range of spacelike scales  $0 < \mu^2 < \infty$ . The pQCD coupling  $a(\mu^2)$  has Landau singularities (in the range  $0 < \mu^2 < 1 \text{ GeV}^2$ ), and hence a regularisation of the resummed result is needed. We further perform evaluation of the resummed result by using holomorphic (analytic) couplings  $\mathcal{A}(\mu^2)$ , where no regularisation is needed.

In Sec. II we present the theoretical OPE expression for inelastic BSR  $\bar{\Gamma}_1^{\text{p-n}}(Q^2)$  and discuss its structure. In Sec. III we construct a renormalon-based extension of the expansion of the QCD canonical part of BSR,  $d(Q^2)$ , to all orders of the coupling. On the basis of these results, we construct in Sec. IV the characteristic function of  $d(Q^2)$  and describe the corresponding resummation for the cases of the pQCD running coupling  $a(\mu^2)$  and of holomorphic coupling  $\mathcal{A}(\mu^2)$ . These results are entirely independent of the renormalisation scale. We discuss the renormalisation scheme dependence of these results in Sec. V, where we also explore numerical behaviour of  $d(Q^2)$  when it is resummed, or has a form of approximants based on truncated information, either in pQCD or in variants of QCD with holomorphic coupling (AQCD). We then use all these results in Sec. VI to evaluate the (truncated) OPE and fit it to the experimental data, and thus we extract the values of the OPE  $D = 2$  and  $D = 4$  coefficients, both in the case when the pQCD coupling is used and when two types of the (AQCD) holomorphic coupling are used. Finally, in Sec. VII we discuss the obtained numerical results and summarise the work. Some formal details used in this work are given in Appendices A-F.

A short version of the analysis with pQCD coupling, but without a systematic analysis with AQCD couplings, appeared in Ref. [18]. In this context, we point out that the present work contains an extended version, with more explanatory details, of the analysis of our previous work [18] for the analysis with the pQCD coupling (cf. also the new Appendices A-E) and the results of that analysis are unchanged [Eqs. (45) and (47) here]. Apart from extending the work of Ref. [18], the present paper presents and emphasises the systematic analysis with various AQCD couplings and the corresponding results that are not contained in Ref. [18]. The detailed pQCD formulation is included in the present work in order to be as transparent and pedagogical as possible and in order to be able to make comparisons between the results of the formalisms using AQCD and pQCD couplings.

## II. THEORETICAL EXPRESSIONS

The polarised Bjorken sum rule (BSR),  $\bar{\Gamma}_1^{\text{p-n}}$ , is defined as the difference between the Ellis-Jaffe sum rule for proton ( $\bar{\Gamma}_1^p$ ) and neutron ( $\bar{\Gamma}_1^n$ ) that involve integration over the Bjorken scaling variable  $x$  of the polarised structure functions  $g_1^N(x, Q^2)$  ( $N = p, n$ ) of the deep inelastic electron-nucleon scattering (DIS)

$$\bar{\Gamma}_1^{\text{p-n}}(Q^2) = \int_0^{1^-} dx [g_1^p(x, Q^2) - g_1^n(x, Q^2)]. \quad (1)$$

Here  $Q^2 = -q^2$  and  $q^2 = (q^0)^2 - \vec{q}^2$  is the square of the transferred DIS momentum. Only the inelastic part was taken (i.e.,  $x \neq 1$ ), this is indicated notationally as the bar over  $\Gamma$  and the  $1^-$  integral limit.

Relatively good experimental data for  $g_1^N(x, Q^2)$  ( $N = p, n$ ) and thus for  $\bar{\Gamma}_1^{\text{p-n}}(Q^2)$  are available [3–10] for the range  $0 < Q^2 < 5 \text{ GeV}^2$  [ $(2\bar{m}_c)^2 \approx 6.5 \text{ GeV}^2$ ]. Therefore, we will consider the charm quark mass to be decoupled in the first approximation, i.e., we will use massless three-flavour QCD ( $N_f = 3$ ) and we will subsequently add the charm quark nondecoupling corrections.

The theoretical expression for BSR (1) is Operator Product Expansion (OPE) [1, 2]

$$\bar{\Gamma}_1^{\text{p-n, OPE}}(Q^2) = \left| \frac{g_A}{g_V} \right| \frac{1}{6} [1 - d(Q^2) - \delta d(Q^2)_{m_c}] + \sum_{i=2}^{\infty} \frac{\mu_{2i}(Q^2)}{Q^{2i-2}}. \quad (2)$$

Here,  $|g_A/g_V|$  is the ratio of the nucleon axial charge, and we take the value  $|g_A/g_V| = 1.2754$  [19]. The quantity  $d(Q^2)$  is the canonical dimension zero ( $D = 0$ ) QCD part with  $N_f = 3$ , and it has perturbation expansion in powers of the (pQCD) coupling  $a(Q^2) \equiv \alpha_s(Q^2)/\pi$

$$d(Q^2)_{\text{pt}} = a(Q^2) + d_1 a(Q^2)^2 + d_2 a(Q^2)^3 + d_3 a(Q^2)^4 + \mathcal{O}(a^5), \quad (3)$$

where  $d_0 = 1$ . In the  $\overline{\text{MS}}$  scheme,  $a(Q^2) = a^{\overline{\text{MS}}}(Q^2)$  and  $d_j = d_j^{\overline{\text{MS}}}$ , and the first four coefficients  $d_j^{\overline{\text{MS}}}$  ( $j = 0, 1, 2, 3$ ) are exactly known and were obtained in [11–13]. The next coefficient  $d_4^{\overline{\text{MS}}}$  can be estimated by the effective charge (ECH) method [20], and its value in the 5-loop  $\overline{\text{MS}}$  scheme is  $d_4^{\overline{\text{MS}}} = 1557.4$ . Therefore,

$$d_4^{\overline{\text{MS}}} = d_4^{\overline{\text{MS}}}(\text{ECH}) \pm 32.8 \approx 1557.4 \pm 32.8, \quad (4)$$

where the uncertainty  $\pm 32.8$  was obtained by the following argument: for the value  $d_4^{\overline{\text{MS}}} = 1557.4 - 32.8 = 1524.6$ , and in the preferred renormalisation scheme [P44-scheme with  $c_2 = 9$ . and  $c_3 = 20$ ., see Eqs. (35)-(36)], the Borel transform  $\mathcal{B}[\tilde{d}](u)$  gives zero  $u=-2$  UV renormalon contribution, i.e.,  $\tilde{d}_2^{\text{UV}} = 0$ ., cf. Sec. III.

The  $D = 2$  term in the OPE (2) has a specific and known  $Q^2$ -dependence

$$\frac{\mu_4(Q^2)}{Q^2} = \frac{M_N^2}{9} \frac{[(a_2^{\text{P-n}} + 4d_2^{\text{P-n}}) + 4\bar{f}_2 a(Q^2)^{k_1}]}{Q^2}, \quad (5)$$

where the anomalous dimension of the corresponding operator is  $k_1 = 32/81$  [21], the nucleon mass is  $M_N = 0.9389$  GeV, and  $(a_2^{\text{P-n}} + 4d_2^{\text{P-n}}) \approx 0.063$  is a combination of the twist-2 target correction  $a_2^{\text{P-n}} \approx 0.031$  and of a twist-3 matrix element

$$d_2^{\text{P-n}} = \int dx x^2 (2g_1^{\text{P-n}} + 3g_2^{\text{P-n}}) (\approx 0.008). \quad (6)$$

The value of the dimensionless parameter  $\bar{f}_2$ , and possibly of the coefficient  $\mu_6$  at the  $D = 4$  OPE term, are to be determined by the fitting of the theoretical expression (2) to the BSR experimental values. Due to the lack of theoretical knowledge,  $\mu_6$  will be considered to be  $Q^2$ -independent. The OPE (2) will be truncated either at  $D = 2$  ( $i = 2$ ) or  $D = 4$  ( $i = 3$ ) term.

The term  $\delta d(Q^2)_{m_c}$  in Eq. (2) is the correction due to the non-decoupling of the charm mass (i.e.,  $m_c \neq \infty$  effects). This term is known up to  $\mathcal{O}(a^2)$  [22] and can be written as

$$\delta d(Q^2)_{m_c} = \frac{1}{6} \left[ \ln \left( \frac{Q^2}{m_c^2} \right) - 2C_{\text{pBJ}}^{\text{mass.},(2)} \left( \frac{Q^2}{m_c^2} \right) \right] a(Q^2)^2 + \mathcal{O}(a^3). \quad (7)$$

Here,  $m_c$  is the pole mass of the charm quark ( $m_c \approx 1.67$  GeV [19]); the expression for  $C_{\text{pBJ}}^{\text{mass.},(2)}(\xi)$  was obtained in [22]; the logarithmic term above is obtained from the difference of  $a(Q^2)$  for  $N_f = 4$  and  $N_f = 3$ . We refer to Appendix A for more details (cf. also App. E of [15]).

### III. RENORMALON STRUCTURE

We follow the approach of Ref. [23] to describe and model the renormalon structure of BSR, specifically of the QCD canonical part of BSR,  $d(Q^2)$ , appearing in the OPE (2). The first step in this Section is to construct a new Borel transform  $\mathcal{B}[\tilde{d}](u)$  and to highlight its relation with the usual Borel transform of  $d(Q^2)$ ,  $\mathcal{B}[d](u)$ . Then, in the next Section, we use  $\mathcal{B}[\tilde{d}](u)$  to obtain the so called characteristic function of  $d(Q^2)$  and the corresponding resummed expression for  $d(Q^2)$ .

The usual perturbation expansion of  $d(Q^2)$  is in powers of the coupling  $a(\mu^2)$ , where  $\mu^2 = \kappa Q^2$  is a chosen renormalisation scale ( $0 < \kappa \lesssim 1$ )

$$d(Q^2) = a(\kappa Q^2) + d_1(\kappa)a(\kappa Q^2)^2 + \dots + d_n(\kappa)a(\kappa Q^2)^{n+1} + \dots \quad (8)$$

We recall that  $d(Q^2)$  is  $\kappa$ -independent because BSR is an observable. The usual Borel transform of  $d(Q^2)$ ,  $\mathcal{B}[d](u; \kappa)$ , is the generating function of the above perturbation coefficients  $d_n(\kappa Q^2)$

$$\mathcal{B}[d](u; \kappa)_{\text{ser}} \equiv 1 + \frac{d_1(\kappa)}{1!\beta_0} u + \dots + \frac{d_n(\kappa)}{n!\beta_0^n} u^n + \dots, \quad (9)$$

and the inverse Borel transformation is

$$d(Q^2) = \frac{1}{\beta_0} \int_0^\infty du \exp \left[ -\frac{u}{\beta_0 a(\kappa Q^2)} \right] \mathcal{B}[d](u; \kappa). \quad (10)$$

The series (8) in powers  $a(\kappa Q^2)^n$  can be reorganised into a series in logarithmic derivatives  $\tilde{a}_n(\kappa Q^2)$

$$\tilde{a}_n(\mu^2) \equiv \frac{(-1)^{n-1}}{(n-1)!\beta_0^{n-1}} \left( \frac{d}{d \ln \mu^2} \right)^{n-1} a(\mu^2) \quad (n = 1, 2, \dots). \quad (11)$$

Here,  $\beta_0 = (11 - 2N_f/3)/4$  ( $\beta_0 = 9/4$  when  $N_f = 3$ ) is the one-loop beta-coefficient in the renormalisation group equation (RGE)

$$\frac{da(\mu^2)}{d \ln \mu^2} = -\beta_0 a(\mu^2)^2 - \beta_1 a(\mu^2)^3 - \beta_2 a(\mu^2)^4 - \beta_3 a(\mu^2)^5 - \dots \quad (12a)$$

$$= -\beta_0 a(\mu^2)^2 [1 + c_1 a(\mu^2) + c_2 a(\mu^2)^2 + c_3 a(\mu^2)^3 + \dots]. \quad (12b)$$

As a consequence, we have  $\tilde{a}_n(\mu^2) = a(\mu^2)^n + \mathcal{O}(a^{n+1})$ . The series (8) in powers  $a(\kappa Q^2)^n$  is then reorganised into a series of these logarithmic derivatives  $\tilde{a}_n(\kappa Q^2)$ , giving

$$d(Q^2) = a(\kappa Q^2) + \tilde{d}_1(\kappa) \tilde{a}_2(\kappa Q^2) + \dots + \tilde{d}_n(\kappa) \tilde{a}_{n+1}(\kappa Q^2) + \dots, \quad (13)$$

where the corresponding expansion coefficients are denoted as  $\tilde{d}_n(\kappa)$ . If we know all the beta-coefficients  $c_j$  of the RGE Eq. (12b),<sup>2</sup> we can explicitly express each of the new coefficients  $\tilde{d}_n(\kappa)$  as a linear combination of the original coefficients  $d_n(\kappa), d_{n-1}(\kappa), \dots$ , cf. Appendix B for explicit relations up to  $n = 4$ . Further, the inverse relations can be constructed as well, i.e., each  $d_n(\kappa)$  is a linear combination of  $\tilde{d}_n(\kappa), \tilde{d}_{n-1}(\kappa), \dots$ , cf. Appendix B.<sup>3</sup>

We define the new Borel transform  $\mathcal{B}[\tilde{d}](u; \kappa)$  by replacing in the usual Borel transform  $\mathcal{B}[d](u; \kappa)$ , Eq. (9), the coefficients  $d_n(\kappa) \mapsto \tilde{d}_n(\kappa)$

$$\mathcal{B}[\tilde{d}](u; \kappa)_{\text{ser}} \equiv 1 + \frac{\tilde{d}_1(\kappa)}{1! \beta_0} u + \dots + \frac{\tilde{d}_n(\kappa)}{n! \beta_0^n} u^n + \dots \quad (14)$$

It turns out that the  $\kappa$ -dependence of the coefficients  $\tilde{d}_n(\kappa)$  and of the Borel transform  $\mathcal{B}[\tilde{d}](u; \kappa)$  is significantly simpler than that of  $d_n(\kappa)$  and  $\mathcal{B}[d](u; \kappa)$

$$\frac{d}{d \ln \kappa} \tilde{d}_n(\kappa) = n \beta_0 \tilde{d}_{n-1}(\kappa) \quad \Rightarrow \quad (15a)$$

$$\mathcal{B}[\tilde{d}](u; \kappa) = \kappa^u \mathcal{B}[\tilde{d}](u), \quad (15b)$$

where we denoted, for simplicity,  $\mathcal{B}[\tilde{d}](u, \kappa = 1) \equiv \mathcal{B}[\tilde{d}](u)$ . This  $\kappa$ -dependence is a direct consequence of the  $\kappa$ -independence of the (canonical) BSR  $d(Q^2)$ , as shown in Appendix C. We point out that the relations Eqs. (15) are not in the one-loop or large- $\beta_0$  approximation, but are exact. Eqs. (15a) can be integrated; as a consequence,  $\tilde{d}_0(\kappa) = 1$  is  $\kappa$ -independent, and  $\tilde{d}_n(\kappa)$  for  $n \geq 1$  has a relatively compact expression in terms of  $\ln \kappa$

$$\tilde{d}_n(\kappa) = \tilde{d}_n + \sum_{k=1}^n \binom{n}{k} (\beta_0 \ln \kappa)^k \tilde{d}_{n-k} \quad (n \geq 1), \quad (16)$$

where we denoted, for simplicity,  $\tilde{d}_n(\kappa = 1) \equiv \tilde{d}_n$ . While the relations (15), for the coefficients  $\tilde{d}_n$  and for  $\mathcal{B}[\tilde{d}](u; \kappa)$ , are exact, we note that for the coefficients  $d_n(\kappa)$  and  $\mathcal{B}[d](u; \kappa)$  the relations of the type (15) are valid only in the one-loop approximation (i.e., when the beta-coefficients are  $\beta_j \mapsto 0$  for  $j = 1, 2, \dots$ ). These relations suggest that the renormalon structure of  $\mathcal{B}[\tilde{d}](u; \kappa)$  is very similar to the large- $\beta_0$  structure of  $\mathcal{B}[d](u; \kappa)$  (for the latter see [25, 26], cf. also [27, 28]). Therefore, our ansatz for  $\mathcal{B}[\tilde{d}](u; \kappa)$ , at  $\kappa = 1$ , will be

$$\mathcal{B}[\tilde{d}](u) = \exp(\tilde{K}u) \pi \left\{ \tilde{d}_1^{\text{IR}} \frac{1}{(1-u)^{\xi_1}} + \tilde{d}_2^{\text{IR}} \frac{1}{(2-u)} + \tilde{d}_1^{\text{UV}} \frac{1}{(1+u)} + \tilde{d}_2^{\text{UV}} \frac{1}{(2+u)} \right\}, \quad (17)$$

Here,  $\xi_1 = 1 - k_1$ , where  $k_1 = 32/81$  is the mentioned anomalous dimension of the  $D = 2$  OPE term Eq. (5). The large- $\beta_0$  expression for  $\mathcal{B}[d](u; \kappa)$  is also of the above form, except that  $\xi_1 \mapsto 1$  there [25, 26]. In our ansatz for  $\mathcal{B}[\tilde{d}](u)$ , Eq. (17), we have  $\xi_1 \neq 1$  because we know the exact anomalous dimension  $k_1$  of the  $D = 2$  OPE term. On the other hand, for the  $D = 2\ell \geq 4$  OPE terms only the large- $\beta_0$  (LB) value of the anomalous dimension  $k_\ell$  is known,  $k_\ell^{(\text{LB})} = 0$

<sup>2</sup> The renormalisation scheme is parametrised by the coefficients  $c_j$  ( $j = 2, 3, \dots$ ) [24]. The coefficients  $c_1 = \beta_1/\beta_0 = (1/4)(102 - 38N_f/3)/(11 - 2N_f/3)$  and  $\beta_0 = (1/4)(11 - 2N_f/3)$  are universal in mass independent schemes.

<sup>3</sup> Note that we have  $d_0(\kappa) = \tilde{d}_0(\kappa) = 1$ .

TABLE I: The values of  $\tilde{K}$  and of the renormalon residues  $\tilde{d}_j^X$  ( $X=IR,UV$ ), for the ansatz (17) in various  $N_f = 3$  renormalisation schemes: 5-loop  $\overline{MS}$ ; P44  $\overline{MS}$  (i.e., with  $c_2 = c_2^{\overline{MS}} = 4.47106$  and  $c_3 = c_3^{\overline{MS}} = 20.9902$ ); P44 with  $c_2 = 9.$  &  $c_3 = 20.$ ; and P44 LMM (i.e.,  $c_2 = c_2^{\text{LMM}} = 9.29703$  and  $c_3 = c_3^{\text{LMM}} = 71.4538$ ). See Sec. V for P44 schemes. In all these schemes,  $d_4$  of  $d(Q^2)$  is taken such that it corresponds to  $d_4^{\overline{MS}} = 1557.43$  in the 5-loop  $\overline{MS}$ . The last line is for the 5-loop  $\overline{MS}$  with  $d_4^{\overline{MS}} = 1557.43 - 32.84 = 1524.59$ , cf. Eq. (4), for which  $\tilde{d}_2^{UV} \approx 0$ .

scheme	$\tilde{K}$	$\tilde{d}_1^{IR}$	$\tilde{d}_2^{IR}$	$\tilde{d}_1^{UV}$	$\tilde{d}_2^{UV}$
$\overline{MS}$ (5-loop)	-1.82336	7.81560	-14.8199	-0.0413348	-0.0920349
$\overline{MS}$ (P44)	-1.83223	7.86652	-14.9299	-0.0444416	-0.0776748
$c_2 = 9.$ & $c_3 = 20.$ (P44)	0.450041	0.331813	0.231437	-0.0809782	-0.0964868
LMM (P44)	0.443075	0.0726314	0.880932	-0.0086770	-0.372221
$d_4^{\overline{MS}} = 1524.6$	0.528239	0.276962	0.283465	-0.100381	$\mathcal{O}(10^{-5})$

(i.e.,  $\xi_\ell = 1 - k_\ell = 1$ ). We will explain below why the infrared pole multiplicity indices  $\xi_\ell$  in the above expression for  $\mathcal{B}[\tilde{d}](u)$  ( $\ell = 1, 2$ ) and the OPE anomalous dimensions  $k_\ell$  have the general relation  $\xi_\ell = 1 - k_\ell$  ( $\ell = 1, 2$ ).

The expression (17) then generates, via the expansion (14), the coefficients  $\tilde{d}_n \equiv \tilde{d}_n(\kappa = 1)$ . The expression (17) has altogether five parameters: the rescaling parameter  $\tilde{K}$  and the residues  $\tilde{d}_1^{IR}, \tilde{d}_2^{IR}, \tilde{d}_1^{UV}, \tilde{d}_2^{UV}$ . These five parameters are determined uniquely from the knowledge the first five coefficients  $d_n$  (and thus  $\tilde{d}_n$ ), i.e., for  $n = 0, 1, 2, 3, 4$ . The resulting numerical values are presented in Table I, in various renormalisation schemes: 5-loop  $\overline{MS}$  scheme, and three P44-type schemes that are explained later on in Sec. V.

When the renormalisation scale parameter  $\kappa$  is varied from  $\kappa = 1$  to values  $\kappa \neq 1$ , the Borel transform (17) changes simply according to the relation (15b)

$$\mathcal{B}[\tilde{d}](u; \kappa) = \exp\left((\ln \kappa + \tilde{K})u\right) \pi \left\{ \tilde{d}_1^{IR} \frac{1}{(1-u)^{\xi_1}} + \tilde{d}_2^{IR} \frac{1}{(2-u)} + \tilde{d}_1^{UV} \frac{1}{(1+u)} + \tilde{d}_2^{UV} \frac{1}{(2+u)} \right\}. \quad (18)$$

It can be checked that, when starting from this expression Eq. (18) and using the known values of the coefficients  $\tilde{d}_n(\kappa)$  ( $n = 0, \dots, 4$ ), we extract the same values of  $\tilde{K}, \tilde{d}_1^{IR}, \tilde{d}_2^{IR}, \tilde{d}_1^{UV}, \tilde{d}_2^{UV}$  as with the analogous approach using Eq. (17) and the corresponding values of the coefficients  $\tilde{d}_n \equiv \tilde{d}_n(\kappa = 1)$ . This is a manifestation of the consistency of our approach.

The terms  $\sim 1/(p \pm u)^\xi$  in the ansatz (17) for  $\mathcal{B}[\tilde{d}](u)$  can be shown to correspond to the following terms in the usual Borel transform  $\mathcal{B}[d](u)$  [23, 29]:

$$\mathcal{B}[\tilde{d}](u)_{\pm p} = \frac{A}{(p \mp u)^\xi} \Rightarrow \quad (19a)$$

$$\mathcal{B}[d](u)_{\pm p} = \frac{B}{(p \mp u)^{\xi \pm p\beta_1/\beta_0^2}} [1 + \mathcal{O}(p \mp u)], \quad (19b)$$

The terms Eq. (19b) represent the theoretically expected renormalon structures of the usual Borel transform  $\mathcal{B}[d](u)$  [26].

When the infrared renormalon term  $\sim 1/(p-u)^{\xi+p\beta_1/\beta_0^2}$ , Eq. (19b), appearing in the Borel transform  $\mathcal{B}[d](u)$ , is Borel-resummed according to Eq. (10), the  $Q^2$ -dependence of the so called renormalon ambiguity is obtained

$$\delta d(Q^2)_{p,\xi} \sim \frac{1}{\beta_0} \text{Im} \int_{+i\epsilon}^{+\infty+i\epsilon} du \exp\left(-\frac{u}{\beta_0 a(Q^2)}\right) \frac{1}{(p-u)^{\xi+p\beta_1/\beta_0}} \quad (20a)$$

$$\sim \frac{1}{(Q^2)^p} a(Q^2)^{1-\xi} [1 + \mathcal{O}(a)]. \quad (20b)$$

This renormalon ambiguity should have the same  $Q^2$ -dependence as the  $D = 2p$  OPE terms of the full observable BSR (2). In view of Eqs. (5) and (17), this implies that  $\xi_1 = 1 - k_1 (= 1 - 32/81)$ , as mentioned earlier. We will take  $\mu_6$  as  $Q^2$ -independent in the OPE (2) because we do not know the exact anomalous dimension of the corresponding operator; therefore,  $k_2 = 0$  and  $\xi_2 = 1 - k_2 = 1$ , implying that the term  $1/(2-u)^{\xi_2}$  in Eq. (17) has index  $\xi_2 = 1$ .

#### IV. RESUMMATION

In this Section we use the knowledge of the new Borel transform  $\mathcal{B}[\tilde{d}](u; \kappa)$  of the (canonical  $D = 0$  part of) BSR  $d(Q^2)$ , Eqs. (18) and (14), in order to perform the resummation of this quantity  $d(Q^2)$ . We follow again the approach presented in [23].

The main element of this approach lies in the fact that the resummation of  $d(Q^2)$  can be written in the form

$$d(Q^2)_{\text{res}} = \int_0^\infty \frac{dt}{t} F_d(t) a(tQ^2), \quad (21)$$

which involves the running QCD coupling  $a(Q'^2)$  and a so called characteristic function  $F_d(t)$  of  $d(Q^2)$ . It turns out that this characteristic function  $F_d(t)$  is related directly to the new Borel transform  $\mathcal{B}[\tilde{d}](u; \kappa)$  presented in the previous Section, cf. Eqs. (14) and (18).

The construction of  $F_d(u)$  goes as follows. In the integral (21) we perform Taylor-expansion of  $a(tQ^2)$  around the (spacelike) squared momentum  $\mu^2 = \kappa Q^2$  (the relevant variable is the logarithm of the squared momenta)

$$a(tQ^2) = a(\kappa Q^2) + (-\beta_0) \ln(t/\kappa) \tilde{a}_2(\kappa Q^2) + \dots + (-\beta_0)^n \ln^n(t/\kappa) \tilde{a}_{n+1}(\kappa Q^2) + \dots \quad (22)$$

When we exchange the order of integration and summation, and we take into account that in the expansion of  $d(Q^2)$  in the logarithmic derivatives  $\tilde{a}_{n+1}(\kappa Q^2)$  the expansion coefficients are  $\tilde{d}_n(\kappa)$ , Eq. (13), we obtain a series of relations (i.e., requirements) for the characteristic function  $F_d(t)$

$$\tilde{d}_n(\kappa) = (-\beta_0)^n \int_0^\infty \frac{dt}{t} F_d(t) \ln^n \left( \frac{t}{\kappa} \right) \quad (n = 0, 1, 2, \dots). \quad (23)$$

When we multiply Eq. (23) by  $u^n/(n!\beta_0^n)$  and sum over  $n$ , we obtain on the left-hand side the new Borel transform  $\mathcal{B}[\tilde{d}](u; \kappa)$  according to Eq. (14), and on the right-hand side we exchange the order of integration and summation and thus obtain

$$\mathcal{B}[\tilde{d}](u; \kappa) = \int_0^\infty \frac{dt}{t} F_d(t) \sum_{n=0}^\infty \frac{1}{n!} [-u \ln(t/\kappa)]^n \Rightarrow \quad (24a)$$

$$\mathcal{B}[\tilde{d}](u; \kappa) = \int_0^\infty \frac{dt}{t} F_d(t) t^{-u} \kappa^u. \quad (24b)$$

When we take into account the relation (15b), the common factor  $\kappa^u$  on both sides of relation (24b) cancels out, leading to the  $\kappa$ -independent relation

$$\mathcal{B}[\tilde{d}](u) = \int_0^\infty \frac{dt}{t} F_d(t) t^{-u}, \quad (25)$$

which means that  $\mathcal{B}[\tilde{d}](u)$  is simply the Mellin transform of  $F_d(t)$ . Stated otherwise, the sought for characteristic function  $F_d(t)$  of the observable  $d(Q^2)$  is the inverse Mellin transform of  $\mathcal{B}[\tilde{d}](u)$

$$F_d(t) = \frac{1}{2\pi i} \int_{u_0 - i\infty}^{u_0 + i\infty} du \mathcal{B}[\tilde{d}](u) t^u. \quad (26)$$

Here,  $u_0$  is any value close to zero where the Mellin transform (25) exists. Thus, for BSR we have  $-1 < u_0 < +1$ .

As seen here, the construction of the resummation (21) of  $d(Q^2)$  is based on the (assumed) knowledge of the given coefficients  $\tilde{d}_n(\kappa)$  of the expansion (13) at any fixed chosen value of  $\kappa$  [i.e., on the knowledge of  $\mathcal{B}[\tilde{d}](u; \kappa)$ , e.g., Eq. (15b)], but the obtained characteristic function is  $\kappa$ -independent as is the resummation (21) of  $d(Q^2)$ .

The exponential factor  $\exp(\tilde{K}u)$  in  $\mathcal{B}[\tilde{d}](u)$  of Eq. (17) reflects itself only in a rescaling of the variable in the characteristic function  $F_d(t)$  Eq. (26)

$$F(t)_d = G_d(t')|_{t'=t \exp(\tilde{K})}, \quad (27)$$

where  $G_d(t')$  is the characteristic function for the case when we set  $\tilde{K} = 0$  in  $\mathcal{B}[\tilde{d}](u)$  of Eq. (17). Hence we can rewrite the resummed expression (21) in the following form (we denote  $t' = t \exp(\tilde{K})$  as new  $t$ ):

$$d(Q^2)_{\text{res}} = \int_0^\infty \frac{dt}{t} G_d(t) a(te^{-\tilde{K}} Q^2), \quad (28)$$

where

$$G_d(t) = \frac{1}{2\pi i} \int_{u_0 - i\infty}^{u_0 + i\infty} du \mathcal{B}[\tilde{d}](u)|_{\tilde{K} \rightarrow 0} t^u, \quad (29)$$

and  $-1 < u_0 < +1$ . For each of the four terms  $\mathcal{B}[\tilde{d}](u)|_{\tilde{K} \rightarrow 0}$  [cf. Eq. (17)] these integrals can be evaluated with application of variants of the Cauchy theorem, cf. [23] and App. C of [29]<sup>4</sup>

$$G_d(t) = \Theta(1-t)\pi \left[ \frac{\tilde{d}_1^{\text{IR}} t}{\Gamma(1-k_1) \ln^{k_1}(1/t)} + \tilde{d}_2^{\text{IR}} t^2 \right] + \Theta(t-1)\pi \left[ \frac{\tilde{d}_1^{\text{UV}}}{t} + \frac{\tilde{d}_2^{\text{UV}}}{t^2} \right], \quad (30)$$

where we recall that  $k_1 = 1 - \xi_1 = 32/81$ . We verified numerically that this expression, in conjunction with Eq. (27), gives us for the integrals on the right-hand side of Eq. (23) the correct values of  $\tilde{d}_n(\kappa)$  as generated by the Borel transform (18).

If we employ in the resummation (28) the pQCD coupling  $a(Q'^2) \equiv \alpha_s(Q'^2)/\pi$ , this coupling has (unphysical) Landau singularities at low positive  $Q'^2$ . In the integration (28), these singularities (cuts) have to be avoided. Therefore, we use the PV-type of regularisation

$$d(Q^2)_{\text{res}} = \text{Re} \left[ \int_0^\infty \frac{dt}{t} G_d(t) a(te^{-\tilde{K}} Q^2 + i\varepsilon) \right]. \quad (31)$$

On the other hand, we can also use a corresponding holomorphic IR-safe coupling  $a(Q^2) \mapsto \mathcal{A}(Q^2)$ , i.e., a coupling that has no Landau singularities but practically coincides with  $a(Q^2)$  at large  $|Q^2| > \Lambda_{\text{QCD}}^2$ . For example, such are the 2 $\delta$ AQCD [31, 32] or 3 $\delta$ AQCD couplings [33, 34]. In such a case, no regularisation is needed in the resummation (28)

$$d(Q^2)_{\text{res,AQCD}} = \int_0^\infty \frac{dt}{t} G_d(t) \mathcal{A}(te^{-\tilde{K}} Q^2). \quad (32)$$

In Sec. VI, we will fit the OPE expression (2), with terms up to dimension  $D = 4$  ( $i = 3$ ) included, to experimental data for BSR  $\bar{\Gamma}_1^{\text{p-n}}(Q^2)$ , where in the OPE we evaluate the QCD canonical part  $d(Q^2)$  either with the pQCD resummation Eq. (31) or AQCD resummation Eq. (32).

## V. RENORMALISATION SCHEME DEPENDENCE

The described method of resummation, Eqs. (31)-(32), is independent of the renormalisation scale parameter  $\kappa = \mu^2/Q^2$ . However, it is not independent of the renormalisation scheme, which is parametrised by the beta-function coefficients  $(c_2, c_3, \dots)$  appearing in the RGE (12b). This is so because our extraction approach of the (five) parameters  $\tilde{K}$  and  $\tilde{d}_j^{\text{X}}$  ( $j = 1, 2; \text{X}=\text{IR}, \text{UV}$ ) ensures the reproduction of the first known five terms  $\tilde{d}_n(\kappa; c_2, \dots, c_n) \tilde{a}_{n+1}(\kappa; c_2, \dots)$  ( $0 \leq n \leq 4$ ) when the resummed expression Eq. (31) is re-expanded in  $\tilde{a}_{n+1}(\kappa; c_2, \dots)$ , implying that we should expect

$$\frac{\partial}{\partial c_j} d(Q^2)_{\text{res}} = \mathcal{O}(\tilde{a}_6) = \mathcal{O}(a^6) \quad (j = 2, 3, \dots) \quad (33)$$

and analogous relation in holomorphic QCD (AQCD) resummation Eq. (32)

$$\frac{\partial}{\partial c_j} d(Q^2)_{\text{res,AQCD}} = \mathcal{O}(\tilde{\mathcal{A}}_6) = \mathcal{O}(a^6) \quad (j = 2, 3, \dots). \quad (34)$$

The explicit dependence of the coefficients  $\tilde{d}_n(\kappa)$  ( $n \leq 4$ ) on the scheme parameters  $c_j$  ( $j \geq 2$ ) is given in Appendix D. While one would expect that  $\mathcal{O}(\tilde{a}_6)$  are small, the (pQCD) quantity  $\tilde{a}_6(Q^2)$ , or  $a(Q^2)^6$ , is not necessarily small at

---

<sup>4</sup> In App. C of [29] the characteristic function was obtained for the terms in  $\mathcal{B}[\tilde{d}](u)$  of the form  $1/(3-u)^\xi$  and  $1/(2-u)^\xi$  (for  $0 < \xi \leq 1$ ), but the derivation for the case of  $1/(1-u)^\xi$  can be performed analogously. See also [30].

low scales  $Q^2 \lesssim 1 \text{ GeV}^2$ . Furthermore, the coefficients  $d_n$  and  $\tilde{d}_n$  are expected to grow very fast when  $n$  increases (e.g., for  $n \geq 5$ ) because of the IR renormalon at  $u = p = 1$ :  $\tilde{d}_n \sim (n+1)!(\beta/p)^n$  where  $p = 1$ .

In this context, we wish to stress that our expression (17) for  $\mathcal{B}[\tilde{d}](u)$ , which generates all the coefficients  $\tilde{d}_n$  (also those with  $n \geq 5$ ) is expected to be only approximate, because: (a) the term  $\sim 1/(1-u)^{\xi_1}$  is expected to have also subleading terms (corrections)  $\sim 1/(1-u)^{\xi_1-1}$ ; (b) the other terms in Eq. (17) are expected to have noninteger power indices related to the (unknown) anomalous dimensions beyond the large- $\beta_0$  approximation, but we took for those terms the large- $\beta_0$  approximation there.

We can see in Table I another practical indication that the scheme dependence is important, by comparing the values of the extracted parameters  $\tilde{K}$  and  $\tilde{d}_j^X$  ( $j = 1, 2$ ; X=IR, UV) in two P44-type schemes:<sup>5</sup> P44  $\overline{\text{MS}}$  (with  $c_2 = \bar{c}_2 = 4.471$  and  $c_3 = \bar{c}_3 = 20.99$ ); and P44 with  $c_2 = 9$  &  $c_3 = 20$ . In the case of P44  $\overline{\text{MS}}$ , the two IR residue parameters  $\tilde{d}_1^{\text{IR}}$  and  $\tilde{d}_2^{\text{IR}}$  are large and of opposite signs, leading to strong cancellations of the corresponding two IR contributions to the resummed expression  $d(Q^2)_{\text{res}}$  Eq. (31), and thus possible numerical instabilities in the evaluation of  $d(Q^2)_{\text{res}}$ . This is not so in the P44 scheme with  $c_2 = 9$  &  $c_3 = 20$ ., where the two IR contributions are smaller, mutually comparable and of the same sign.

For all these reasons, we will vary the scheme parameters in specific convenient ranges. Further, we will restrict ourselves to a class of schemes, namely the so called P44-class which allows an explicit (and thus convenient) solution of the RGE (12) for the running coupling  $a(Q^2)$ . The beta-function in this class has only two adjustable scheme parameters, namely the two leading scheme parameters  $c_2$  and  $c_3$  (while  $c_j$ 's for  $j \geq 4$  are then specific functions of  $c_2$  and  $c_3$ ). Such a beta-function  $\beta(a)$  has a Padé form [4/4](a) ('P44'), i.e., it is a ratio of two polynomials of degree 4 in  $a(Q^2)$

$$\frac{da(Q^2)}{d \ln Q^2} = \beta(a(Q^2)) \equiv -\beta_0 a(Q^2)^2 \frac{[1 + \alpha_0 c_1 a(Q^2) + \alpha_1 c_1^2 a(Q^2)^2]}{[1 - \alpha_1 c_1^2 a(Q^2)^2][1 + (\alpha_0 - 1)c_1 a(Q^2) + \alpha_1 c_1^2 a(Q^2)^2]}, \quad (35)$$

where  $c_j \equiv \beta_j/\beta_0$  and

$$\alpha_0 = 1 + \sqrt{c_3/c_1^3}, \quad \alpha_1 = c_2/c_1^2 + \sqrt{c_3/c_1^3}. \quad (36)$$

When we expand this  $\beta$ -function in powers of  $a(Q^2)$ , the terms up to the (four-loop) term with  $c_3$  of the expansion (12b) are reproduced, while the terms with  $c_j$  ( $j \geq 4$ ) have the coefficients  $c_j$  as specific functions of  $c_2$  and  $c_3$ . The RGE (35) has explicit solution in terms of the Lambert functions  $W_{\mp 1}(z)$ , as shown in [35]

$$a(Q^2) = \frac{2}{c_1} \left[ -\sqrt{\omega_2} - 1 - W_{\mp 1}(z) + \sqrt{(\sqrt{\omega_2} + 1 + W_{\mp 1}(z))^2 - 4(\omega_1 + \sqrt{\omega_2})} \right]^{-1}, \quad (37)$$

where  $\omega_1 = c_2/c_1^2$ ,  $\omega_2 = c_3/c_1^3$ ,  $Q^2 = |Q^2| \exp(i\phi)$ , and  $W_{\mp 1}(z)$  are two branches of the Lambert function. When  $0 \leq \phi < \pi$ ,  $W_{-1}(z)$  is used; when  $-\pi \leq \phi < 0$ ,  $W_{+1}(z)$  is used. The argument  $z = z(Q^2)$  appearing in  $W_{\pm 1}(z)$  is

$$z \equiv z(Q^2) = -\frac{1}{c_1 e} \left( \frac{\Lambda_L^2}{Q^2} \right)^{\beta_0/c_1}. \quad (38)$$

We call the scale  $\Lambda_L$  appearing here the Lambert scale; it turns out that  $\Lambda_L^2 \sim \Lambda_{\text{QCD}}^2$  ( $\sim 0.1 \text{ GeV}^2$ ). The scale convention in all these schemes is the same as in  $\overline{\text{MS}}$ , only the chosen scheme parameters ( $c_2, c_3$ ) are now in general different than those in  $\overline{\text{MS}}$ . The scale  $\Lambda_L$  is related to the strength of the coupling. We will call the described class of schemes as P44-schemes. They are all for the  $N_f = 3$  case, i.e., QCD with three massless quarks (and the other quarks are considered decoupled).

The strength of the coupling Eq. (37), or equivalently the scale  $\Lambda_L$ , is determined by the value of  $\alpha_s^{\overline{\text{MS}}}(M_Z^2)$ . This is obtained in the following way. We RGE-evolve  $a(Q^2) \equiv \alpha_s(Q^2)/\pi$  from  $Q^2 = M_Z^2$  (where  $N_f = 5$ ) with the 5-loop  $\overline{\text{MS}}$  RGE [36] downwards, and take the corresponding 4-loop quark threshold relations [37, 38] at  $Q^2 = k\bar{m}_q$  (we take  $k = 2$ ;  $\bar{m}_b = 4.2 \text{ GeV}$ ;  $\bar{m}_c = 1.27 \text{ GeV}$ ). Then at a scale  $Q^2 = Q_0^2$  and  $N_f = 3$  (we took  $Q_0^2 = (2\bar{m}_c)^2 - 0$ ) we change the scheme from the 5-loop  $\overline{\text{MS}}$  to the mentioned P44-scheme with chosen  $c_2$  and  $c_3$  values, via the relation

<sup>5</sup> See later in this Section the explanation of the P44-type schemes.



(cf. App. A of [24] and App. A of [39])

$$\begin{aligned} \frac{1}{a} + c_1 \ln \left( \frac{c_1 a}{1 + c_1 a} \right) + \int_0^a dx \left[ \frac{\beta(x) + \beta_0 x^2 (1 + c_1 x)}{x^2 (1 + c_1 x) \beta(x)} \right] \\ = \frac{1}{\bar{a}} + c_1 \ln \left( \frac{c_1 \bar{a}}{1 + c_1 \bar{a}} \right) + \int_0^{\bar{a}} dx \left[ \frac{\bar{\beta}(x) + \beta_0 x^2 (1 + c_1 x)}{x^2 (1 + c_1 x) \bar{\beta}(x)} \right], \end{aligned} \quad (39)$$

where  $a = a(Q_0^2)$  is the coupling in the chosen (P44) scheme,  $\bar{a} = \bar{a}(Q_0^2)$  is the coupling in the 5-loop  $\overline{\text{MS}}$  scheme obtained by the aforementioned RGE-evolution, and  $\bar{\beta}(x)$  is the 5-loop  $\overline{\text{MS}}$  beta-function (polynomial), all with  $N_f = 3$ . The above relation (39) is solved numerically to obtain the value of  $a = a(Q_0^2)$  in the P44 scheme with chosen  $c_2$  and  $c_3$ . From here, using Eq. (37) (with  $Q^2 = Q_0^2$ ) and the relation (38), we obtain the value of  $\Lambda_L$ . Then we can obtain  $a(Q^2)$  at any other  $Q^2$  (and keeping  $N_f = 3$ ) by the formula (37).

On the other hand, as mentioned earlier, the transformation of the expansion coefficients  $\tilde{d}_n$  of BSR  $d(Q^2)$  under the change of the scheme is presented in App. D. Incidentally, we can see in Table I that the extracted values of the parameters of the Borel transform  $\mathcal{B}[\tilde{d}](u)$  in the 5-loop  $\overline{\text{MS}}$  and in the P44  $\overline{\text{MS}}$  are very similar to each other. This is so because these two schemes differ only starting at the 5-loop level (i.e., the  $c_4$  value differs in the two schemes). As mentioned earlier, these two schemes are not preferred because of strong cancellations of the IR  $u = 1$  (IR1) and IR  $u = 2$  (IR2) contributions to  $d(Q^2)$  that lead to possible numerical instabilities.

Therefore, we will confine ourselves to such P44-schemes where the various contributions to  $d(Q^2)_{\text{res}}$ , Eq. (31), behave in the following way:

1. The contribution  $d(Q^2)_{\text{IR1}}$ , from IR  $u = 1$  term, is the dominant contribution.
2. The rescaling parameter  $\tilde{K}$  in  $\mathcal{B}[\tilde{d}](u)$  is  $|\tilde{K}| < 1$ .
3. We restrict the contribution  $d(Q^2)_{\text{IR2}}$  to:  $0 < d(Q^2)_{\text{IR2}} < d(Q^2)_{\text{IR1}}$ .
4. The contribution  $d(Q^2)_{\text{UV2}}$ , from UV  $u = -2$ , is restricted to be not too large:  $|\tilde{d}_2^{\text{UV}}| < 0.5$ .

It turns out that the conditions 2. and 3. are often related: namely, when  $d(Q^2)_{\text{IR2}} < 0$ , we usually have  $|\tilde{K}| > 1$ , and  $d(Q^2)_{\text{IR1}}$  and  $d(Q^2)_{\text{IR2}}$  are large and with opposite signs, leading to strong cancellation in  $d(Q^2)_{\text{res}}$ . Further, it has been shown in [40, 41] that the assumption of the dominance of the  $u = 1$  renormalon (IR1) (in the  $\overline{\text{MS}}$  scheme) in BSR gives a good prediction of the known coefficient  $d_3$ . Under the conditions given above, we obtain what we regard as an acceptable range of (P44)-scheme parameters

$$c_2 = 9_{-1.4}^{+2}, \quad c_3 = 20 \pm 15. \quad (40)$$

If  $c_2$  decreased below the value  $(9 - 1.4) = 7.6$ , the value of  $|\tilde{K}|$  would grow suddenly and would lead to strong cancellation of the  $d(Q^2)_{\text{IR1}}$  and  $d(Q^2)_{\text{IR2}}$  contributions.

The results for the values of the parameters of the Borel transform  $\mathcal{B}[\tilde{d}](u)$  are presented in Table II for various P44-schemes consistent with the range Eq. (40) - for the central case and for the cases when one parameter ( $c_2$ , or  $c_3$ ) has the minimal or maximal allowed value. Furthermore, in Table II we present also the corresponding various numerical contributions to the resummed canonical BSR  $d(Q^2)_{\text{res}}$  of Eq. (31). For comparison, we include in Table II the cases of the P44 LMM (Lambert MiniMOM, see below) and P44  $\overline{\text{MS}}$  schemes, where for these two schemes the conditions (40) are not satisfied.

In Fig. 1 we present these resummed values  $d(Q^2)_{\text{res}}$  as a function of  $Q^2$ , for the considered central case of P44-scheme ( $c_2 = 9$ . and  $c_3 = 20$ ). The value of the Lambert scale of the coupling is taken to be  $\Lambda_L = 0.21745$  GeV, this corresponds to the value  $\alpha_s^{\overline{\text{MS}}}(M_Z^2) = 0.1179$ .

For comparison, we include also the values of  $d(Q^2)_{\text{res};\text{AQCD}}$  Eq. (32) for the central cases of the two holomorphic QCD variants  $2\delta\text{AQCD}$  and  $3\delta\text{AQCD}$ , i.e., with couplings  $\mathcal{A}(Q^2)$  that have no Landau singularities. The QCD variant  $2\delta\text{AQCD}$  is in the P44-scheme with  $c_2 = 9$ . and  $c_3 = 20$ ., and the variant  $3\delta\text{AQCD}$  is in the (lattice-related) Lambert MiniMOM (LMM) P44-scheme [42–45].<sup>6</sup> The construction of these QCD variants is explained in Appendix

<sup>6</sup> The (P44) LMM scheme ( $c_2^{\text{LMM}} = 9.29703$  and  $c_3^{\text{LMM}} = 71.4538$ ) is tied to  $3\delta\text{AQCD}$  and must be used there, cf. Appendix F. This scheme fulfills the mentioned conditions 2 and 4, has no cancellation effects in the IR sector, but instead of the condition 3 has:  $0 < d(Q^2)_{\text{IR1}} < d(Q^2)_{\text{IR2}}$ .

TABLE II: The parameter values of the Borel transform (17) in the P44 schemes, for the values of the scheme parameters  $c_2$  and  $c_3$  covering the range Eq. (40). Presented are also the corresponding numerical values of the canonical BSR  $d(Q^2)$  and its separate four renormalon contributions, for the resummation (31) at  $Q^2 = 3 \text{ GeV}^2$  (and  $N_f = 3$ ) and for  $\alpha_s^{\overline{\text{MS}}}(M_Z^2) = 0.1179$ . We further include the cases of P44 LMM ( $c_2^{\text{LMM}} = 9.29703$  and  $c_3^{\text{LMM}} = 71.4538$ ) and P44  $\overline{\text{MS}}$  schemes ( $c_2^{\overline{\text{MS}}} = 4.47106$  and  $c_3^{\overline{\text{MS}}} = 20.9902$ ), where the conditions (40) are not fulfilled. In all the cases, the coefficient  $d_4$  corresponds to coefficient value  $d_4(\overline{\text{MS}}) = 1557.43$  in the 5-loop  $\overline{\text{MS}}$ , cf. Eq. (4).

$c_2$	$c_3$	$\tilde{K}$	$\tilde{d}_1^{\text{IR}}$	$\tilde{d}_2^{\text{IR}}$	$\tilde{d}_1^{\text{UV}}$	$\tilde{d}_2^{\text{UV}}$	$d(Q^2)$	$d(Q^2)_{\text{IR1}}$	$d(Q^2)_{\text{IR2}}$	$d(Q^2)_{\text{UV1}}$	$d(Q^2)_{\text{UV2}}$
9.	20.	0.450041	0.331813	0.231437	-0.0809782	-0.0964868	0.1816	0.1631	0.0597	-0.0247	-0.0164
7.6	20.	0.896252	0.210843	0.137235	-0.158441	0.394581	0.1843	0.1196	0.0421	-0.0551	0.0777
11.0	20.	0.12894	0.422324	0.301175	-0.015641	-0.477922	0.1807	0.1904	0.0701	-0.0044	-0.0752
9.	5.	0.359327	0.474866	-0.026115	-0.080151	-0.126694	0.1737	0.2243	-0.0064	-0.0236	-0.0207
9.	35.	0.484948	0.237256	0.431189	-0.067963	-0.133156	0.1888	0.1188	0.1143	-0.0212	-0.0232
$c_2^{\text{LMM}}$	$c_3^{\text{LMM}}$	0.443075	0.072631	0.880932	-0.008677	-0.372221	0.1741	0.0345	0.2060	-0.0027	-0.0638
$c_2^{\overline{\text{MS}}}$	$c_3^{\overline{\text{MS}}}$	-1.83223	7.86652	-14.9299	-0.044442	-0.077675	0.1632	1.9466	-1.7675	-0.0082	-0.0076

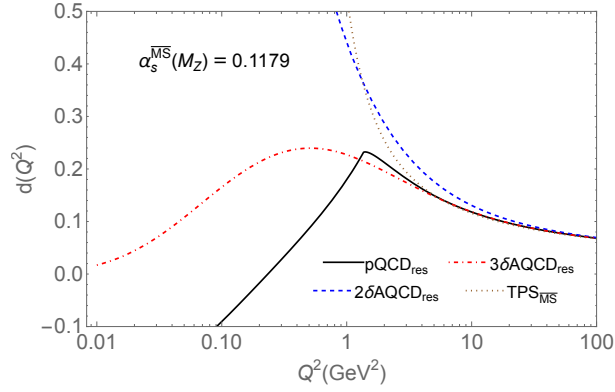


FIG. 1: The resummed canonical part of BSR,  $d(Q^2)_{\text{res}}$  (at  $N_f = 3$ ), according to Eq. (31), in the P44 renormalisation scheme with  $c_2 = 9.$  and  $c_3 = 20.$ , for  $N_f = 3$  ('pQCD<sub>res</sub>'). The strength of the coupling is determined by the choice  $\alpha_s(M_Z^2; \overline{\text{MS}}) = 0.1179$ . The resummations with the corresponding  $2\delta\text{AQCD}$  and  $3\delta\text{AQCD}$  coupling are included, for comparison (' $2\delta\text{AQCD}_{\text{res}}$ ', ' $3\delta\text{AQCD}_{\text{res}}$ '). Further, we include the evaluation as the truncated perturbation series (TPS) in powers of  $a = a(Q^2)$  in  $\overline{\text{MS}}$  scheme, up to  $\sim a^5$  term ('TPS $_{\overline{\text{MS}}}$ '). All involved couplings correspond to the strength  $\alpha_s^{\overline{\text{MS}}}(M_Z^2; N_f = 5) = 0.1179$ , and the  $d_4$  coefficient value corresponds to the central value Eq. (4) of the corresponding  $\overline{\text{MS}}$  coefficient,  $d_4^{\overline{\text{MS}}} = 1557.4$ .

F, and they are used also in the numerical fits later on in Sec. VI. In both these holomorphic cases the strength of the underlying pQCD coupling  $a(Q'^2)$  corresponds to  $\alpha_s^{\overline{\text{MS}}}(M_Z^2) = 0.1179$ , and the threshold mass of the spectral function of the coupling  $\mathcal{A}(Q'^2)$  has the chosen value  $M_1 = 0.150 \text{ GeV}$ . We refer to Appendix F for more details.

As seen in Fig. 1, the curve for the pQCD case has a (soft) kink at  $Q^2 \approx 1.44 \text{ GeV}^2$ . Such kinks do not appear in the cases of AQCD. The reason for the kink are the Landau singularities of the pQCD coupling  $a(te^{-\tilde{K}Q^2} + i\epsilon)$  in the integrand of the resummation (31) at low  $tQ^2$ , and the effect of these singularities becomes rather abruptly more pronounced when  $Q^2$  has lower values ( $Q^2 \leq 1.44 \text{ GeV}^2$ ). Furthermore, we see in Fig. 1 that the curve of  $d(Q^2)$  for  $2\delta\text{AQCD}$  converges to the asymptotic (pQCD) behaviour at quite high  $Q^2$  (in contrast to the  $3\delta\text{AQCD}$  curve); this is related to the fact that the  $2\delta\text{AQCD}$  coupling  $\mathcal{A}(Q'^2)$  at low  $Q'^2$  achieves relatively high values (cf. Appendix F) and these contributions are significant in the resummation integral (32) at low  $t$  values, even when  $Q^2$  is relatively high. We remark that in Fig. 1 the pQCD TPS curve (in  $\overline{\text{MS}}$ , with  $\kappa = 1$ ) becomes infinite at  $Q^2 \approx 0.40 \text{ GeV}^2$ , which is the branching point of the Landau cut of the  $\overline{\text{MS}}$  pQCD coupling; for  $Q^2 < 0.40 \text{ GeV}^2$ , that TPS curve does not exist. On the other hand, the  $2\delta\text{AQCD}$  and  $3\delta\text{AQCD}$  curves in Fig. 1 remain finite all the way down to  $Q^2 = 0$  (where they reach the values of 3.70 and zero, respectively).

We present in Figs. 2(a) and 3(a) the results for  $d(Q^2)$  in  $2\delta\text{AQCD}$  and  $3\delta\text{AQCD}$  in the resummed form (32) and compare them to the truncated "perturbation" series in logarithmic derivatives in those models, i.e., AQCD analogs of the series Eq. (13) as presented in Appendix F, Eqs. (F5)-(F6), with  $\kappa = 1$  and truncated at  $\sim \tilde{\mathcal{A}}_N$

$$d(Q^2)_{\text{AQCD}}^{[N]} = \mathcal{A}(Q^2) + \tilde{d}_1 \tilde{\mathcal{A}}_2(Q^2) + \dots + \tilde{d}_{N-1} \tilde{\mathcal{A}}_N(Q^2), \quad (41)$$

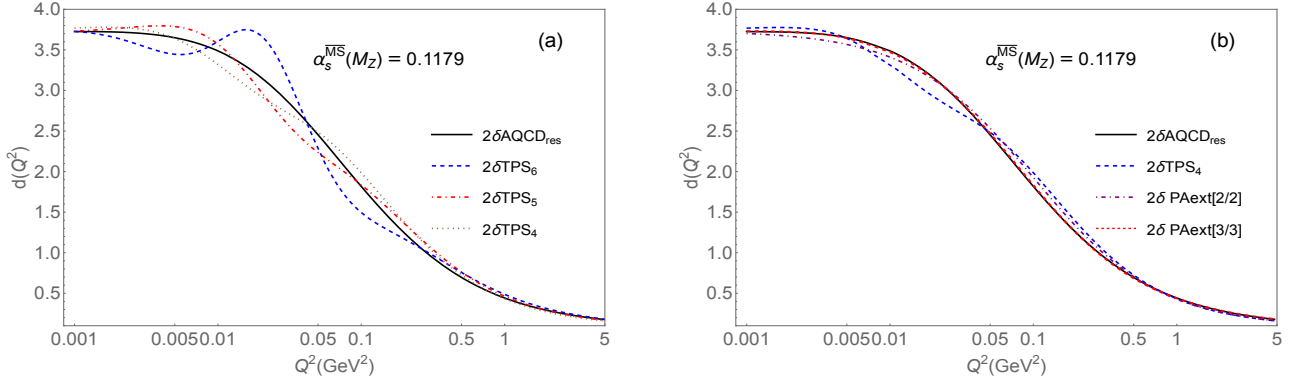


FIG. 2: The resummed  $d(Q^2)$  in  $2\delta\text{AQCD}$ , compared with various approximants based on truncated information about the coefficients  $\tilde{d}_n$  ( $n \leq 5$ ): (a) the truncated series  $d(Q^2)_{2\delta\text{AQCD}}^{[N]}$  (41) (' $2\delta\text{TPS}_N$ ') for  $N = 4, 5, 6$ ; (b) the Padé-related renormalisation scale-invariant approximants  $\mathcal{G}_d^{[M/M]}(Q^2)_{2\delta\text{AQCD}}$  Eq. (F7) (' $2\delta\text{PAext}[M/M]$ '), for  $M = 2$  and  $M = 3$ . Input parameters for the coupling are  $\alpha_s^{\overline{\text{MS}}}(M_Z^2) = 0.1179$  and  $M_1 = 0.150$  GeV. The value of the coefficient  $d_4$  corresponds to  $d_4^{\overline{\text{MS}}} = 1557.4$ . We note that the  $2\delta\text{PAext}[3/3]$  curve practically (visually) coincides with the resummed curve.

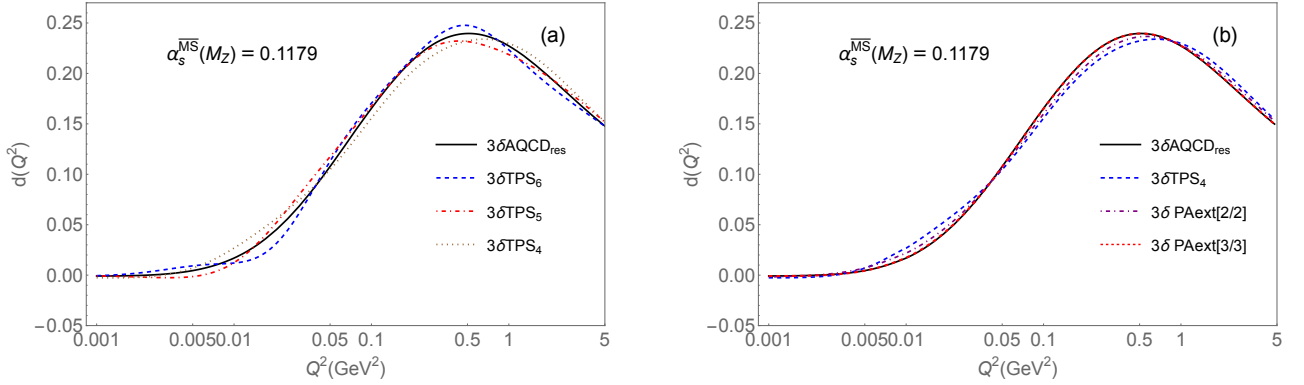


FIG. 3: The same as in Figs. 2, but in  $3\delta\text{AQCD}$  (instead of  $2\delta\text{AQCD}$ ). We note that the  $3\delta\text{PAext}[3/3]$  curve practically (visually) coincides with the resummed curve.

where we denoted as earlier, for simplicity,  $\tilde{d}_n(\kappa = 1) \equiv \tilde{d}_n$ . We note that formally,  $\tilde{\mathcal{A}}_N \sim a^N$  where  $a$  is the underlying pQCD coupling. We can observe in Fig. 2(a), and to a lesser degree in 3(a), numerical indications that the truncated AQCD series (41) give us a divergent sequence when the truncation index  $N$  increases (in the figures we have  $4 \leq N \leq 6$ ), i.e., we have no convergence to the resummed curves when  $N$  increases.

On the other hand, in Figs. 2(b) and 3(b) we include the curves of the Padé-related approximants  $\mathcal{G}_d^{[M/M]}(Q^2)_{\text{AQCD}}$  (denoted as 'PAext[M/M]': 'extensions' of (diagonal) Padé's). The approximants were introduced in the framework of pQCD in [46]. They were later applied in QCD variants with holomorphic coupling (AQCD, i.e., free of Landau singularities) in Refs. [23, 47–49]; they were applied there to the (spacelike) Adler function and to related QCD observables. These approximants are briefly explained here in Appendix F [Eqs. (F7)-(F8)]. These approximants are constructed only from the first  $N = 2M$  expansion coefficients  $\tilde{d}_n(\kappa)$  of  $d(Q^2)$  [i.e., from the coefficients  $\tilde{d}_j(\kappa)$ ,  $0 \leq j \leq (2M - 1)$ ], they are entirely independent of the renormalisation scale parameter  $\kappa$ , and they formally approximate  $d(Q^2)$  up to the precision  $\sim \tilde{\mathcal{A}}_{2M+1}$ , i.e., the difference  $[d(Q^2) - \mathcal{G}_d^{[M/M]}(Q^2)_{\text{AQCD}}]$  is  $\sim \tilde{\mathcal{A}}_{2M+1}$  (and this is formally  $\sim a^{2M+1}$ , where  $a$  is the underlying pQCD coupling).<sup>7</sup> We can see in Figs. 2(b) and 3(b) that these approximants converge fast toward the resummed value of  $d(Q^2)$ , Eq. (32), when  $N(= 2M)$  increases. This is in stark

<sup>7</sup> We point out that these approximants  $\mathcal{G}_d^{[M/M]}(Q^2)$  often cannot be applied in pQCD in practice because of the presence of Landau poles in  $a(Q'^2)$  at low positive  $Q'^2$ . In this respect, we note these approximants contain pQCD terms  $\tilde{\alpha}_j a(\kappa_j Q^2)$  for various  $\tilde{\alpha}_j$  and  $\kappa_j > 0$ , and usually some  $\kappa_j$ 's have low values ( $\kappa_j \ll 1$ ), cf. Table V in Appendix F.

contrast to the corresponding truncated series approximants (41) with  $N = 2M$ , cf. Figs. 2(a) and 3(a).

## VI. FITS TO THE EXPERIMENTAL DATA, IN PQCD AND AQCD

The experimental data for inelastic BSR  $\bar{\Gamma}_1^{\text{p-n}}(Q^2)$  have been obtained by various experiments [3–10], for the range  $0 < Q^2 < 5 \text{ GeV}^2$ . They are shown in Figs. 4, where the statistical and systematic uncertainties are also presented.

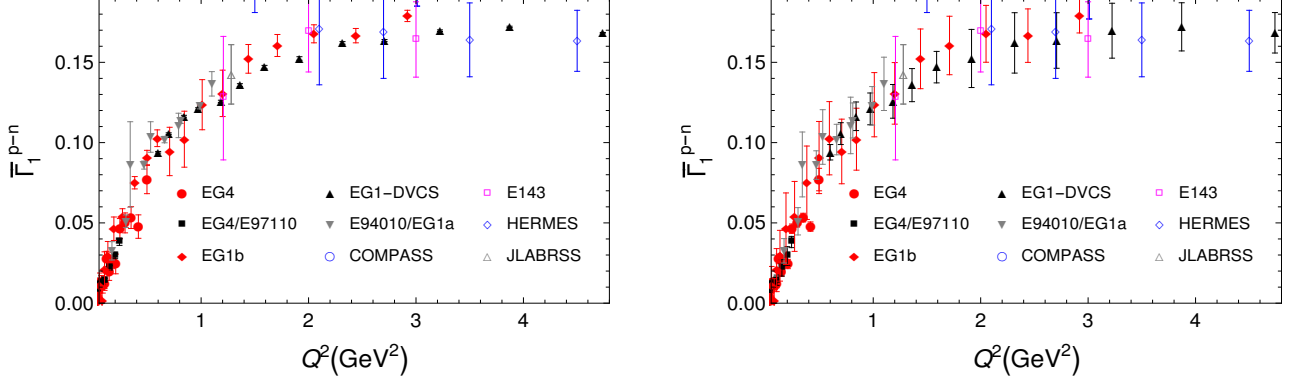


FIG. 4: The experimental values for the inelastic BSR  $\bar{\Gamma}_1^{\text{p-n}}(Q^2)$ , based on the measured values of the polarised structure functions from different experiments. Shown are also the statistical (left Figure) and systematic (right Figure) uncertainties. There are altogether 77 experimental points, at the squared momenta  $Q_j^2$  ( $j = 1, \dots, 77$ ) in increasing order,  $0.021 \text{ GeV}^2 \leq Q_j^2 \leq 4.739 \text{ GeV}^2$ . This figure was presented also in [18].

In the first part of this Section we will present the fit results with the approach using the pQCD coupling, and in the second part the fit results when using the  $2\delta\text{AQCD}$  and  $3\delta\text{AQCD}$  couplings.

### A. Fits with (resummed) pQCD approach

We first perform the fit with pQCD approach, i.e., the above experimental values are fitted with the theoretical OPE expression Eq. (2) truncated either at  $D = 2$  ( $i = 2$ ), or at  $D = 4$  ( $i = 3$ ), and where the QCD canonical part  $d(Q^2)$  is evaluated with the renormalon-based resummation Eq. (31). The running coupling  $a(Q^2)$  is evaluated in massless QCD with  $N_f = 3$  in the P44 renormalisation schemes according to Eq. (37) and with scheme parameters  $c_2$  and  $c_3$  in the range Eq. (40); for the central case we take the central values of Eq. (40),  $c_2 = 9$  and  $c_3 = 20$ . Also the  $m_c \neq \infty$  nondecoupling effects, Eq. (7), are evaluated, for convenience, with such coupling  $a(Q^2)$  [although formally, at  $\sim a^2$ , the choice of the scheme in Eq. (7) is arbitrary]. For the  $a(Q^2)$ -strength parameter, i.e., Lambert scale  $\Lambda_L$  Eq. (38), we take such value that it corresponds to the central world average value  $\alpha_s^{\overline{\text{MS}}}(M_Z^2) = 0.1179$  [19], as explained in the previous Section. The fit consists, in principle, of varying either the one fit parameter  $f_2$ , or the two fit parameters  $f_2$  and  $\mu_6$ , cf. Eqs. (2)-(5), such that the quantity

$$\chi^2(j_{\min}; k) = \frac{1}{(j_{\max} - j_{\min} + 1 - N_p)} \sum_{j=j_{\min}}^{j_{\max}} \frac{[\bar{\Gamma}_1^{\text{p-n, OPE}}(Q_j^2) - \bar{\Gamma}_1^{\text{p-n}}(Q_j^2)_{\text{exp}}]^2}{\sigma(Q_j^2; k)^2} \quad (42)$$

is minimised. Here,  $Q_j^2$  (where:  $j = 1, \dots, j_{\max}$ ;  $j_{\max} = 77$ ) are the squared momentum scales at which the experimental data are available ( $Q_1^2 < Q_2^2 < \dots < Q_{77}^2$ ). Further,  $N_p$  is the number of fit parameters:  $N_p = 1$  if  $\mu_6 = 0$  and  $\bar{f}_2$  is varied;  $N_p = 2$  if both  $f_2$  and  $\mu_6$  are varied. The index parameter  $j_{\min}$  indicates a chosen minimal  $Q_{\min}^2 = Q_{j_{\min}}^2$  scale for which the experimental data are included in the fit; and  $j_{\max} = 77$  corresponds to the maximal fit scale,  $Q_{\max}^2 = Q_{77}^2 = 4.739 \text{ GeV}^2$ . Hence, the interval of scales included in the fit is:  $Q_{j_{\min}}^2 \leq Q^2 \leq 4.739 \text{ GeV}^2$ . The uncorrelated squared uncertainties  $\sigma(Q_j^2; k)^2$  at  $Q_j^2$  in the expression (42) are in principle unknown. The statistical errors  $\sigma_{\text{stat}}(Q_j^2)$  are expected to be largely uncorrelated, but the systematic errors  $\sigma_{\text{sys}}(Q_j^2)$  may have significant, but unknown, correlations. Therefore, we follow here the method of unbiased estimate [50–52]. This method consists of the following. A fraction of  $\sigma_{\text{sys}}^2(Q_j^2)$  is added to  $\sigma_{\text{stat}}^2(Q_j^2)$

$$\sigma^2(Q_j^2; k) = \sigma_{\text{stat}}^2(Q_j^2) + k \sigma_{\text{sys}}^2(Q_j^2). \quad (43)$$

The obtained uncertainties  $\sigma(Q_j^2; k)$  are regarded as uncorrelated, and the mentioned fit parameters (only  $\bar{f}_2$ ; or  $\bar{f}_2$  and  $\mu_6$ ) are extracted by minimisation of the above expression  $\chi^2(j_{\min}; k)$ , Eq. (42), in the mentioned chosen interval of  $Q^2$  values. This process is continued, by adjusting iteratively the parameter  $k$  and minimising  $\chi^2(j_{\min}; k)$  until the value  $\chi^2(j_{\min}; k) = 1$  is obtained. In practice, in this way we always obtain  $0 < k < 0.5$ . We note that the smaller the obtained value of  $k$ , the better is the fit.

The experimental uncorrelated uncertainty (exp.u.) of the obtained fit parameters ( $\bar{f}_2$ ; or  $\bar{f}_2$  and  $\mu_6$ ) is then obtained by the conventional methods as explained, e.g., in App. of Ref. [53], or App. D of [29]. For completeness, we describe this method of obtaining 'exp.u.' in Appendix E.

The experimental correlated uncertainty (exp.c.) is then obtained by simply shifting the central experimental values  $\bar{\Gamma}_1^{p-n}(Q_j^2)_{\text{exp}}$  in the expression (42) by the errors complementary to  $\sigma(Q_j^2; k)$  of Eq. (43), namely by  $(1 - \sqrt{k})\sigma_{\text{sys}}(Q_j^2)$ , up and down, and conducting the minimisation of this new  $\chi^2(j_{\min}; k)$ . The corresponding variation '(exp.c.)' of the extracted parameters is then the difference between such "shifted" extracted values and the central ("unshifted") values.

Another question is how to choose the preferred value of  $Q_{\min}^2$  ( $= Q_{j_{\min}}^2$ ). The results of the fit can depend considerably on the choice of the value of  $Q_{\min}^2$ , and this is clearly true in the considered pQCD approach. In pQCD, our choice is  $Q_{\min}^2 = 1.71 \text{ GeV}^2$  in the fit with two parameters ( $\bar{f}_2, \mu_6$ ), resulting in the  $k$  value  $k = 0.1621$ . The reasons for this choice are the following: 1.) When decreasing  $Q_{\min}^2$  from  $Q_{\min}^2 = 1.71 \text{ GeV}^2$  to the neighbouring lower data points, the value of  $k$  increases (and thus the quality of the fit decreases). It increases from  $k = 0.162$  (for  $Q_{\min}^2 = 1.71 \text{ GeV}^2$ ) to  $k = 0.172, 0.201$  (for  $Q_{\min}^2 = 1.59, 1.50 \text{ GeV}^2$ ). When decreasing  $Q_{\min}^2$  one step further (to  $1.44 \text{ GeV}^2$ ), then the evaluation of  $d(Q^2)$ , via Eq. (31), comes very close to the border of applicability at such  $Q^2$ . This border of applicability is due to the Landau singularities of the pQCD coupling, and it is manifested in Fig. 1 as a soft kink in the (resummed pQCD) curve at about  $Q^2 \approx 1.44 \text{ GeV}^2$ .<sup>8</sup> 2.) On the other hand, when we increase  $Q_{\min}^2$  above  $1.71 \text{ GeV}^2$  to the next upper neighbouring point  $1.915 \text{ GeV}^2$ , the value of  $k$  increases moderately to  $k = 0.180$ ; however, when increasing further, strong cancellations between the resulting  $D = 2$  and  $D = 4$  terms appear. Therefore, we choose  $Q_{\min}^2 = 1.71_{-0.27}^{+0.205} \text{ GeV}^2$ . We recall that the central value of the  $k$  parameter is  $k = 0.1621$ .

When the fit in pQCD is made with only one fit parameter ( $\bar{f}_2$ ), similar reasoning leads us to the similar range  $Q_{\min}^2 = 1.71_{-0.27}^{+0.39} \text{ GeV}^2$ , and the corresponding central value of the  $k$  parameter is  $k = 0.1487$ .<sup>9</sup>

To summarise, we obtain for  $Q_{\min}^2$

$$(Q_{\min}^2)^{(\text{pQCD}),2\text{p}} = 1.71_{-0.27}^{+0.205} \text{ GeV}^2, \quad (44\text{a})$$

$$(Q_{\min}^2)^{(\text{pQCD}),1\text{p}} = 1.71_{-0.27}^{+0.39} \text{ GeV}^2, \quad (44\text{b})$$

where the superscript '2p' means two-parameter fit, and '1p' one-parameter fit.

The described fits, in the case of the two-parameter fit, give us (cf. Ref. [18])  $k = 0.1621$  and the following results for the two fit parameters:

$$\begin{aligned} \bar{f}_2 = & -0.160_{+0.025}^{-0.007}(c_2)_{-0.039}^{+0.054}(c_3)_{-0.041}^{+0.044}(\alpha_s)_{+0.016}^{-0.012}(d_4) \mp 0.043(\text{ren}) \\ & +_{+0.119}^{+0.016}(Q_{\min}^2) \pm 0.160(\text{exp.u.}) \pm 0.297(\text{exp.c.}), \end{aligned} \quad (45\text{a})$$

$$\begin{aligned} \mu_6 = & +0.022_{-0.008}^{+0.003}(c_2)_{+0.004}^{-0.013}(c_3)_{+0.008}^{-0.010}(\alpha_s)_{-0.003}^{+0.002}(d_4) \mp 0.010(\text{ren}) \\ & -_{-0.053}^{+0.006}(Q_{\min}^2) \pm 0.062(\text{exp.u.}) \mp 0.059(\text{exp.c.}) [\text{GeV}^4]. \end{aligned} \quad (45\text{b})$$

We note that the parameter  $\bar{f}_2$  that appears in the  $D = 2$  OPE term Eq. (5) is dimensionless, but the  $D = 4$  OPE parameter  $\mu_6$  is in units of  $\text{GeV}^4$ . In the results (45), the uncertainties at '( $c_2$ )' and '( $c_3$ )' originate from the renormalisation scheme variation, Eq. (40). The uncertainty at '( $\alpha_s$ )' originates from the world average  $\alpha_s$ -uncertainty  $\alpha_s^{\overline{\text{MS}}}(M_Z^2) = 0.1179 \pm 0.0009$  [19]. The uncertainty at '( $d_4$ )' is from the variation of the values of  $d_4$  (in our central P44 scheme with  $c_2 = 9$ . and  $c_3 = 20$ .) such that the corresponding values of  $d_4$  in the 5-loop  $\overline{\text{MS}}$  scheme vary according to

<sup>8</sup> In the used scheme P44 with  $c_2 = 9$ . and  $c_3 = 20$ . (and  $N_f = 3$ ), and with the strength scale  $\Lambda_L = 0.2175 \text{ GeV}$  corresponding to  $\alpha_s^{\overline{\text{MS}}}(M_Z^2) = 0.1179$ , the Landau cut of  $a(Q'^2)$  is  $0 \leq Q'^2 < 0.87 \text{ GeV}^2$ .

<sup>9</sup> Despite having  $k$  slightly smaller in the one-parameter fit than in the two-parameter fit, the quality of the one-parameter fit is slightly worse than that of the two-parameter fit (as it should be). Namely, we note that the denominator in  $\chi^2(j_{\min}; k)$ , in Eq. (42), depends on the number of fit parameters,  $N_p$ . When this denominator is removed, the resulting sum of squares,  $\bar{\chi}^2(j_{\min}; k)$ , shows that the one-parameter fit is indeed slightly worse than the two-parameter fit [by using in both cases in  $\bar{\chi}^2(j_{\min}; k)$  either  $k = 0.1621$ ; or  $k = 0.1487$ ].

Eq. (4). The uncertainty at '(ren)' comes from the renormalon-type of uncertainty of the resummed results  $d(Q^2)_{\text{res}}$  Eq. (31), i.e., when we add or subtract in the evaluation of  $d(Q^2)_{\text{res}}$  the imaginary part of the same integral (divided by  $\pi$ )

$$\delta d(Q^2)_{\text{ren}} = \pm \frac{1}{\pi} \text{Im} \left[ \int_0^\infty \frac{dt}{t} G_d(t) a(te^{-\bar{K}} Q^2 + i\varepsilon) \right]. \quad (46)$$

In addition to the mentioned five theoretical uncertainties, we have experimental uncertainties. We can regard the uncertainty at ' $(Q_{\text{min}}^2)$ ', which comes from the mentioned variation  $Q_{\text{min}}^2 = 1.71_{-0.27}^{+0.205} \text{ GeV}^2$ , as primarily experimental uncertainty. Furthermore, the uncertainties at '(exp.u.)' and '(exp.c.)' were discussed earlier in this Section. We keep the  $\sigma^2$ -parameter  $k$  fixed at its central value  $k = 0.1621$  all the time, with the exception when  $Q_{\text{min}}^2$  is varied (in that case:  $k = 0.1621_{-0.0247}^{+0.0179}$ ).

In the case when the fit is performed with only one fit parameter ( $\bar{f}_2$ ), the results (cf. Ref. [18]) are  $k = 0.1487$  and

$$\begin{aligned} \bar{f}_2 = & -0.107_{+0.007}^{-0.001}(c_2)_{-0.029}^{+0.022}(c_3) \pm 0.020(\alpha_s) \mp 0.009(d_4) \mp 0.067(\text{ren}) \\ & +_{-0.029}^{+0.012}(Q_{\text{min}}^2) \pm 0.033(\text{exp.u.}) \pm 0.154(\text{exp.c.}). \end{aligned} \quad (47)$$

It turns out that the contribution  $\delta d(Q^2)_{m_c}$  of the violation of the charm quark decoupling, cf. Eq. (7), does not affect strongly the extracted values of parameters. Namely, noninclusion of  $\delta d(Q^2)_{m_c}$  would change the central values in Eqs. (45)  $\bar{f}_2 = -0.160$  to  $-0.165$  (and  $k = 0.1621$  to  $0.1626$ ), and  $\mu_6 = +0.022$  to  $+0.023$ ; and in Eq. (47)  $\bar{f}_2 = -0.107$  to  $-0.108$  (and  $k = 0.1487$  to  $0.1493$ ).

The large experimental uncertainties of the BSR data make the deduction of the preferred value of  $\alpha_s^{\overline{\text{MS}}}(M_Z^2)$  from the BSR data practically impossible. Therefore, we used for  $\alpha_s^{\overline{\text{MS}}}(M_Z^2)$  the world average value [19],  $\alpha_s^{\overline{\text{MS}}}(M_Z^2) = 0.1179 \pm 0.0009$ .

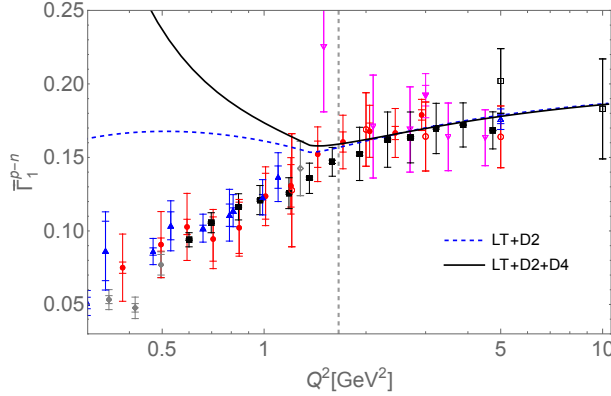


FIG. 5: The fitted curves for the BSR  $\bar{\Gamma}_1^{p-n}(Q^2)$ , for the one-parameter (LT+D2) and two-parameter fits (LT+D2+D4). The coupling used is pQCD. Experimental data are included for comparison. See the text for details. The vertical line indicates the value of the left end of the fit interval for the pQCD curves,  $Q_{\text{min}}^2 = 1.71 \text{ GeV}^2$ .

In Fig. 5 we present the obtained fitted curves  $\bar{\Gamma}_1^{p-n}(Q^2; \bar{f}_2, \mu_6)$  and  $\bar{\Gamma}_1^{p-n}(Q^2; \bar{f}_2)$ , using the OPE expressions (2) with the central fit values of Eqs. (45) and (47). The corresponding central values of the scheme parameters, of  $\alpha_s^{\overline{\text{MS}}}(M_Z^2)$  and of  $d_4$  were used.<sup>10</sup> For comparison, the experimental data are included.

## B. Fits with (resummed) AQCD approach: 2 $\delta$ AQCD, 3 $\delta$ AQCD

In this Section we present analogous results obtained by using variants of QCD with holomorphic couplings [AQCD:  $a(Q^2) \mapsto \mathcal{A}(Q^2)$ ], i.e., with running couplings  $\mathcal{A}(Q^2)$  that have no Landau singularities and the resummation formula

<sup>10</sup> In the contribution  $\delta d(Q^2)_{m_c}$ , Eq. (7), and in the  $D = 2$  OPE contribution, Eq. (5), we freeze the corresponding power  $a(Q^2)^\nu$  ( $\nu = 2, 32/81$ , respectively) for  $Q^2 < 1.5 \text{ GeV}^2$  to the value  $a(1.5)^\nu$ , in order to avoid the problem of vicinity of the Landau singularities there (those singularities are at  $Q^2 < 0.87 \text{ GeV}^2$ ).

(32) can be applied, without any need of regularisation. The employed variants are  $2\delta\text{AQCD}$  [31, 32] and  $3\delta\text{AQCD}$  [33, 34], they are briefly described also here in Appendix F and were mentioned at the end of Sec. V. The renormalisation schemes for  $2\delta\text{AQCD}$  coupling are again taken to be the P44-schemes with the  $c_2$  and  $c_3$  beta-parameters varying in the range (40) as in pQCD; i.e., the central case will be again  $c_2 = 9$ . and  $c_3 = 20$ . On the other hand, the  $3\delta\text{AQCD}$  coupling is related to the large volume lattice results [54, 55] and is thus in a fixed lattice-related scheme, the Lambert MiniMOM (LMM) P44-scheme [42–45] ( $c_2^{\text{LMM}} = 9.2980$  and  $c_3^{\text{LMM}} = 71.4538$ ). As explained in Appendix F, in each of the two mentioned AQCD couplings, the parameters that fix the coupling are two: (a) the value of  $\alpha_s^{\overline{\text{MS}}}(M_Z^2)$  that determines the ( $N_f = 3$ ) scale  $\Lambda_L$  and thus determines the underlying  $N_f = 3$  pQCD coupling; (b) the scale (in GeV) of the lowest threshold mass  $M_1 = \sqrt{\sigma_{\min}}$  of the spectral (discontinuity) function  $\rho(\sigma) = \text{Im}\mathcal{A}(-\sigma - i\epsilon)$ . The threshold scale  $M_1$  is expected to be of the order of the lowest hadronic scale,  $M_1 \sim m_\pi \approx 0.150$  GeV. So, for the central case, we fix the threshold scale to the value  $M_1 = 0.150$  GeV and take  $\alpha_s^{\overline{\text{MS}}}(M_Z^2) = 0.1179$ .

Therefore, repeating the fitting procedure in an analogous way as in the case of pQCD resummation of the previous Sec. VIA, we obtain for the  $2\delta\text{AQCD}$  coupling for the two-parameter fit the values  $k = 0.1330$  and

$$\begin{aligned} \bar{f}_2^{(2\delta)} &= -0.0046_{-0.0106}^{+0.0145}(c_2)_{-0.0145}^{+0.0080}(c_3)_{-0.0464}^{+0.0487}(\alpha_s) \pm 0.0034(d_4)_{+0.0554}^{-0.0764}(M_1) \\ &\quad +_{-0.0231}^{+0.0373}(Q_{\min}^2) \pm 0.0232(\text{exp.u.}) \pm 0.1317(\text{exp.c.}), \end{aligned} \quad (48a)$$

$$\begin{aligned} \mu_6^{(2\delta)} &= +0.0015 \mp 0.0001(c_2)_{-0.0005}^{+0.0007}(c_3)_{+0.0024}^{-0.0027}(\alpha_s) \mp 0.0005(d_4)_{-0.0002}^{-0.0001}(M_1) \\ &\quad -_{+0.0034}^{+0.0073}(Q_{\min}^2) \pm 0.0031(\text{exp.u.}) \mp 0.0149(\text{exp.c.}) [\text{GeV}^4]. \end{aligned} \quad (48b)$$

For the one-parameter fit with  $2\delta\text{AQCD}$  we obtain the values  $k = 0.1283$  and

$$\begin{aligned} \bar{f}_2^{(2\delta)} &= +0.0066_{-0.0095}^{+0.0136}(c_2)_{-0.0183}^{+0.0135}(c_3)_{-0.0281}^{+0.0288}(\alpha_s)_{+0.0003}^{-0.0002}(d_4)_{+0.0542}^{-0.0769}(M_1) \\ &\quad -_{+0.0050}^{+0.0066}(Q_{\min}^2) \pm 0.0038(\text{exp.u.}) \pm 0.0208(\text{exp.c.}). \end{aligned} \quad (49)$$

For the  $3\delta\text{AQCD}$  coupling for the two-parameter fit we obtain the values  $k = 0.1613$  and

$$\begin{aligned} \bar{f}_2^{(3\delta)} &= -0.2531_{-0.0238}^{+0.0244}(\alpha_s)_{+0.0013}^{-0.0014}(d_4)_{-0.0813}^{+0.0766}(M_1) \\ &\quad +_{-0.0128}^{+0.0210}(Q_{\min}^2) \pm 0.0244(\text{exp.u.}) \pm 0.1203(\text{exp.c.}), \end{aligned} \quad (50a)$$

$$\begin{aligned} \mu_6^{(3\delta)} &= +0.0013_{+0.0016}^{-0.0017}(\alpha_s) \pm 0.0002(d_4)_{+0.0046}^{-0.0039}(M_1) \\ &\quad -_{+0.0019}^{+0.0037}(Q_{\min}^2) \pm 0.0032(\text{exp.u.}) \mp 0.0132(\text{exp.c.}) [\text{GeV}^4]. \end{aligned} \quad (50b)$$

For the one-parameter fit with  $3\delta\text{AQCD}$  we obtain the values  $k = 0.1553$  and

$$\begin{aligned} \bar{f}_2^{(3\delta)} &= -0.2430_{-0.0111}^{+0.0113}(\alpha_s)_{-0.0001}^{+0.0001}(d_4)_{-0.0455}^{+0.0472}(M_1) \\ &\quad -_{+0.0022}^{+0.0081}(Q_{\min}^2) \pm 0.0042(\text{exp.u.}) \pm 0.0203(\text{exp.c.}). \end{aligned} \quad (51)$$

As mentioned above, for the  $3\delta\text{AQCD}$  case we cannot present scheme uncertainties (' $c_2$ ') and (' $c_3$ ') because the construction of the  $3\delta\text{AQCD}$  coupling is tied to the lattice (L)MM scheme.

In comparison to the pQCD case, Eqs. (45)-(47), we now have no ('ren') uncertainties coming from the renormalon ambiguity, because no regularisation is needed in the resummation (32). However, the somewhat analogous uncertainty is the (' $M_1$ ') uncertainty in Eqs. (48)-(49) and (50)-(51), which comes by varying the mentioned threshold scale  $M_1$  of the spectral function  $\rho(\sigma)$  of the AQCD coupling; we performed the following variation of this scale:  $M_1 = 0.150_{-0.050}^{+0.100}$  GeV.

Furthermore, the uncertainty (' $Q_{\min}^2$ ') comes now from the following variation, in the  $2\delta\text{AQCD}$  case:

$$(Q_{\min}^2)^{(2\delta)} = 0.592_{-0.122}^{+0.198} \text{ GeV}^2, \quad (52)$$

which is the same in the two-parameter and one-parameter fit. And in the  $3\delta\text{AQCD}$  case the variation is

$$(Q_{\min}^2)^{(3\delta),2p} = 0.592_{-0.096}^{+0.106} \text{ GeV}^2, \quad (53a)$$

$$(Q_{\min}^2)^{(3\delta),1p} = 0.592_{-0.096}^{+0.198} \text{ GeV}^2, \quad (53b)$$

where in the superscripts '2p' and '1p' mean two-parameter and one-parameter fit, respectively. The central values for  $Q_{\min}^2$ , in Eqs. (52)-(53), were obtained in the following way. For each possible  $Q_{\min}^2 = Q_j^2$  ( $1 < j < 77$ ), the fits were performed and the corresponding value of the  $\sigma^2$ -parameter  $k$ , Eq. (43), was obtained. The results are presented

in Figs. 6. The preferred values of  $Q_{\min}^2$  should not be too close to  $Q_{\max}^2 = Q_{77} = 4.739 \text{ GeV}^2$ , in order to have a reasonably wide  $Q^2$ -interval for the fitted experimental values. Since the minimal  $k$  represents the best fit, we choose such  $Q_{\min}^2$  where the approximately minimal value of  $k$  is obtained. This gives the central values of  $Q_{\min}^2$  given above. The variation range of  $Q_{\min}^2$ , as given for each case in Eqs. (52)-(53), was then obtained by requiring that beyond the above ranges a relatively abrupt change (increase) in the value of  $k$  occurs.

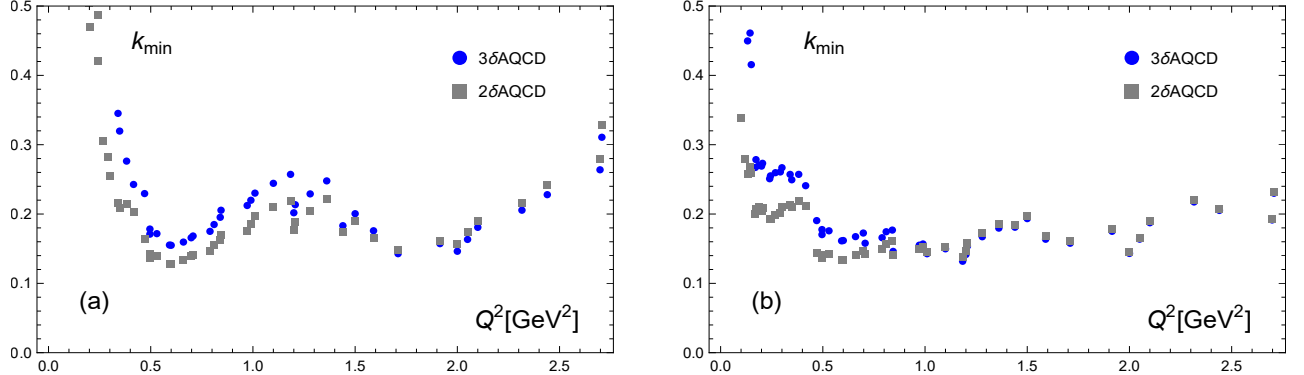


FIG. 6: The values of the  $\sigma^2$ -parameter  $k$ , Eq. (43), for various  $Q^2 = Q_{\min}^2$  for the  $2\delta$  and  $3\delta$ AQCD coupling: (a) when one-parameter fit is performed; (b) when two-parameter fit is performed.

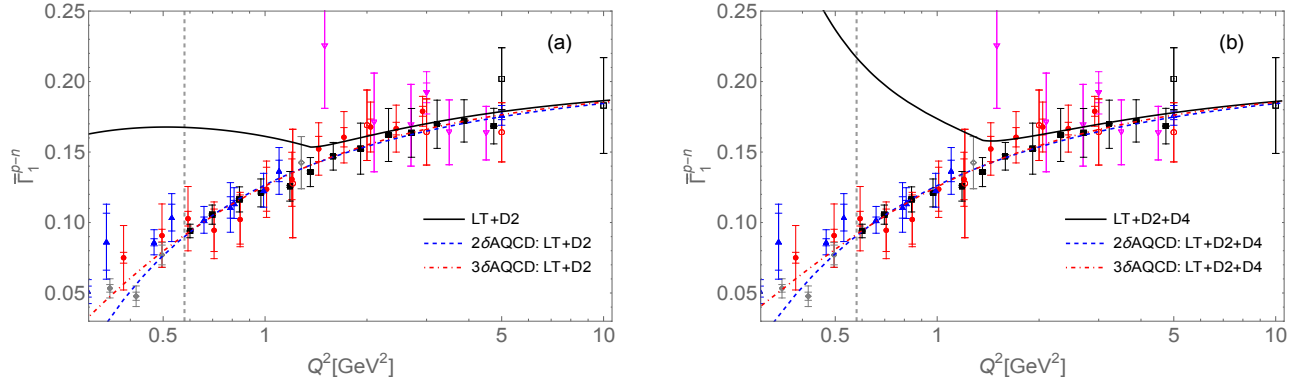


FIG. 7: The fitted curves for the BSR  $\bar{\Gamma}_1^{p-n}(Q^2)$ : (a) for the one-parameter fits; (b) for the two-parameter fits. The couplings used are  $2\delta$ AQCD and  $3\delta$ AQCD. Experimental data, and the corresponding pQCD fit (of Fig. 5; here as solid line), are included for comparison. See the text for details. The vertical line indicates the value of the left end of the fit interval for the AQCD curves,  $Q_{\min}^2 = 0.592 \text{ GeV}^2$ .

In Figs. 7(a), (b), we present the resulting fitting curves  $\bar{\Gamma}_1^{p-n}(Q^2; \bar{f}_2)$  and  $\bar{\Gamma}_1^{p-n}(Q^2; \bar{f}_2, \mu_6)$  for  $2\delta$ AQCD and  $3\delta$ AQCD, using the corresponding central values of parameters of Eqs. (48)-(51). The corresponding central values for the other parameters were used (scheme,  $\alpha_s^{\overline{\text{MS}}}(M_Z^2)$ ,  $M_1$ ,  $d_4$ ).<sup>11</sup> For comparison, the experimental data, and the corresponding pQCD fit (from Fig. 5), are included in the Figures.

## VII. DISCUSSION OF THE RESULTS, AND CONCLUSIONS

In this work, we performed various analyses of the inelastic Bjorken polarised sum rule (BSR). The theoretical basis was the OPE (2) truncated at the dimension  $D = 4$  ( $i = 3$ ) or  $D = 2$  ( $i = 2$ ) term. The canonical leading-twist QCD contribution  $d(Q^2)$  was evaluated by a renormalon-based resummation, Eq. (31) in the case of pQCD coupling  $a(Q'^2)$ ,

<sup>11</sup> In  $\delta d(Q^2)_{m,c}$ , Eq. (7), we used instead of  $a(Q^2)^2$  the AQCD coupling  $\tilde{\mathcal{A}}_2(Q^2)$  ( $\sim a(Q^2)^2$ ); in the  $D = 2$  term, Eq. (5), we used instead of  $a(Q^2)^{k_1}$  the AQCD coupling  $\tilde{\mathcal{A}}_{k_1}(Q^2)$  ( $\sim a(Q^2)^{k_1}$ ).



and Eq. (32) in the case of holomorphic (AQCD) coupling  $\mathcal{A}(Q'^2)$  (i.e., coupling without the Landau singularities) in the  $2\delta$ AQCD and  $3\delta$ AQCD variants of holomorphic QCD. These resummations are completely invariant under the renormalisation scale variation. The obtained theoretical (truncated OPE) expression was then fitted to the available data points for BSR.

In general, the experimental data have too high uncertainties for the extraction of the preferred value of  $\alpha_s^{\overline{\text{MS}}}(M_Z^2)$ , especially when we include the  $D = 4$  term in the OPE. Therefore, we fixed this value to  $\alpha_s^{\overline{\text{MS}}}(M_Z^2) = 0.1179$ , the central world average value [19].<sup>12</sup> The resulting extracted values of the OPE fit parameters  $\bar{f}_2$  and  $\mu_6$  are given for the pQCD case in Eqs. (45)-(47), for the  $2\delta$ AQCD case in Eqs. (48)-(49), and for the  $3\delta$ AQCD case in Eqs. (50)-(51). The various experimental uncertainties of the extracted values are represented by the last three terms there: (' $Q_{\text{min}}^2$ '), (exp.u.) and (exp.c.). We see that the experimental uncertainties are in general the dominant ones, especially the correlated uncertainty (exp.c.). The various theoretical uncertainties are in general smaller, sometimes with the exception of the (' $M_1$ ') uncertainty in AQCD cases, i.e., the uncertainty due to the variation of the spectral function of the holomorphic coupling at low scales  $M_1$ . Furthermore, we see that the use of holomorphic couplings, i.e., when the couplings have no Landau singularities, in general reduces the theoretical and experimental uncertainties of the extracted values by large factors in comparison to the pQCD case, in some cases by one order of magnitude. The (resummed) AQCD results have yet another attractive feature when compared to the (resummed) pQCD results: the preferred fit interval is considerably wider,  $0.592 \text{ GeV}^2 \leq Q^2 \leq 4.739 \text{ GeV}^2$ , than in the pQCD case where it was restricted to  $1.710 \text{ GeV}^2 \leq Q^2 \leq 4.739 \text{ GeV}^2$ . One reason for this is that the pQCD running coupling  $a(Q'^2)$  has Landau cut singularities at low positive values  $Q'^2 \lesssim 1 \text{ GeV}^2$ , while the AQCD couplings  $\mathcal{A}(Q'^2)$  are free of such singularities.

If we apply in the pQCD approach, instead of the resummation (31) in the canonical QCD part  $d(Q^2)$ , a simple truncated power series in  $a(\mu^2)$  (TPS), the results change significantly. For example, the TPS approach in  $\overline{\text{MS}}$  scheme and with  $\alpha_s^{\overline{\text{MS}}}(M_Z^2) = 0.1179$ , leads to significant renormalisation scale dependence, and the truncation index ( $N_{\text{tr}}$ ) dependence.<sup>13</sup> If we choose  $\mu^2 = Q^2$ , the two-parameter fit results are strongly  $N_{\text{tr}}$ -dependent, at  $N_{\text{tr}} = 8$  we obtain small  $\chi^2 = 0.891$  but the values  $\bar{f}_2 \approx -0.44$  and  $\mu_6 = 0.43 \text{ GeV}^4$  are large and lead to significant cancellation effects between  $D = 2$  and  $D = 4$  BSR terms in the range  $2 \text{ GeV}^2 < Q^2 < 3 \text{ GeV}^2$ . On the other hand, for  $N_{\text{tr}} \geq 10$  we obtain very large  $\chi^2 > 4$ . The one-parameter fit results give for all  $N_{\text{tr}} \geq 3$  the values  $\chi^2 > 1$ , and the values of  $\chi^2$  increase when  $N_{\text{tr}}$  increases. These results strongly suggest that the TPS approach in pQCD is less reliable than the (renormalon-based) pQCD resummation approach Eq. (31).

On the other hand, in the holomorphic QCD (i.e., AQCD) the Padé-related approximants  $\mathcal{G}_d^{[M/M]}(Q^2)$ , which are constructed only from the first  $2M$  expansion coefficients  $\tilde{a}_n(\kappa)$  of  $d(Q^2)$ , are completely independent of the renormalisation scale parameter  $\kappa$  and converge rapidly to the fully resummed values of  $d(Q^2)$  of Eq. (32) for all  $Q^2$  when  $M$  increases. These approximants in general do not work well when pQCD coupling is used, due to the Landau singularities of such a coupling.

Our results suggest that for an improved theoretical description of low-energy spacelike observables such as BSR it is important: (a) to perform the fit with resummation of  $d(Q^2)$  according to Eqs. (31) or (32) instead of using truncated expressions; (b) to use, in the resummation, for the running coupling, instead of the pQCD coupling  $a(Q'^2)$ , a holomorphic coupling  $\mathcal{A}(Q'^2)$ , i.e., a coupling that is practically equal to the (underlying) pQCD coupling  $a(Q'^2)$  at high scales  $Q'^2 > 1 \text{ GeV}^2$  and is regulated in the low-scale regime  $Q'^2 \lesssim 1 \text{ GeV}^2$  such that it has no Landau singularities there.

In our work we did not consider models for inelastic BSR  $\bar{\Gamma}_1^{\text{p-n}}(Q^2)$  at very low  $Q^2 < 1 \text{ GeV}^2$ , e.g., expansions [7] motivated on chiral perturbation theory or the light-front holographic QCD (LFH) [56, 57]. In one of our previous works [15] we included such low- $Q^2$  models in the analysis.<sup>14</sup> In the present work, the main emphasis was to construct a renormalon-based extension (to all orders) of the expansion of the canonical BSR part  $d(Q^2)$ , and to resum it with the approach of characteristic function either in the framework of pQCD, Eq. (31), or in the framework of AQCD variants, Eq. (32). With these results, the corresponding OPE was fitted to the experimental data.

We performed numerical analyses (fits) with mathematica software. The mathematica programs that were con-

<sup>12</sup> However, it turns out that in the  $2\delta$ AQCD approach and with OPE truncated at  $D = 2$ , the minimal  $k$  (and thus the best fit) does exist under the variation of  $\alpha_s^{\overline{\text{MS}}}(M_Z^2)$ , and is obtained at  $\alpha_s^{\overline{\text{MS}}}(M_Z^2) = 0.1181$  (and  $\bar{f}_2 = +0.0129$ ;  $k = 0.1280$ ) when the central values of other "input" parameters ( $c_2, c_3, d_4, M_1, Q_{\text{min}}^2$ ) are taken. In the  $3\delta$ AQCD approach, the corresponding preferred value is  $\alpha_s^{\overline{\text{MS}}}(M_Z^2) = 0.1171$  (and  $\bar{f}_2 = -0.253$ ;  $k = 0.1534$ ).

<sup>13</sup> The TPS is truncated at the power  $a(\mu^2)^{N_{\text{tr}}}$ .

<sup>14</sup> The QCD approaches applied in [15] at  $Q^2 \gtrsim 1 \text{ GeV}^2$  for evaluation of  $d(Q^2)$  of BSR were truncated series, either in pQCD or in AQCD variants.

structured and used in the numerical analyses in this work are available on the web page [58], and they include the experimental data.

### Acknowledgments

This work was supported in part by FONDECYT (Chile) Grants No. 1200189 (C.A.) and No. 1220095 (G.C.).

### Appendix A: The effects of $m_c \neq \infty$ in BSR $d(Q^2)$

These effects were evaluated in [22]. We neglect the (heavy)  $b$ -quark contributions (i.e., we consider  $m_b \rightarrow \infty$ ). Then the considered effects, at next-to-leading order (NLO,  $\sim a^2$ ), are expressed with the function  $C_{\text{pBJ}}^{\text{mass.},(2)}(\xi_c)$ . Here,  $\xi_c \equiv Q^2/m_c^2$ . The expression for  $C_{\text{pBJ}}^{\text{mass.},(2)}(\xi_c)$  is valid for  $\xi_c \gtrsim 1$ , and  $m_c \approx 1.67$  GeV is the pole mass. The function  $C_{\text{pBJ}}^{\text{mass.},(2)}$  appears originally in the coefficient at  $a^2$  when the perturbation expansion (3) [or: (8) with  $\kappa = 1$ ], which is for  $N_f = 3$ , is expressed in terms of the  $N_f = 4$  coupling  $a(Q^2)_{N_f=4}$

$$d(Q^2)_{\text{pt}} = a(Q^2)_{N_f=4} + a(Q^2)_{N_f=4}^2 \left\{ \frac{55}{12} - \frac{1}{3} \left[ N_f - 1 + C_{\text{pBJ}}^{\text{mass.},(2)}(\xi_c) \right] \right\} + \mathcal{O}(a^3), \quad (\text{A1})$$

where  $N_f = 4$  and the expression for  $C_{\text{pBJ}}^{\text{mass.},(2)}(\xi_c)$  (when  $\xi_c \equiv Q^2/m_c^2 \gtrsim 1$ ) is

$$C_{\text{pBJ}}^{\text{mass.},(2)}(\xi) = \frac{1}{2520} \left\{ \frac{1}{\xi} (6\xi^2 + 2735\xi + 11724) - \frac{\sqrt{\xi+4}}{\xi^{3/2}} (3\xi^3 + 106\xi^2 + 1054\xi + 4812) \ln \left[ \frac{\sqrt{\xi+4} + \sqrt{\xi}}{\sqrt{\xi+4} - \sqrt{\xi}} \right] \right. \\ \left. - 2100 \frac{1}{\xi^2} \ln^2 \left[ \frac{\sqrt{\xi+4} + \sqrt{\xi}}{\sqrt{\xi+4} - \sqrt{\xi}} \right] + (3\xi^2 + 112\xi + 1260) \ln \xi \right\} \quad (\xi \gtrsim 1). \quad (\text{A2})$$

We note that when  $Q^2 \gg m_c^2$  ( $\xi \gg 1$ ), this function approaches unity quite slowly

$$C_{\text{pBJ}}^{\text{mass.},(2)}(\xi) = 1 - \frac{8}{3} \frac{\ln \xi}{\xi} + \frac{34}{9\xi} + \mathcal{O} \left( \frac{\ln^2 \xi}{\xi^2} \right), \quad (\text{A3})$$

and we obtain the massless  $N_f = 4$  QCD expression for  $d_1$

$$d_1(N_f) = \frac{55}{12} - \frac{1}{3} N_f \quad (\text{A4})$$

with  $N_f = 4$ .

We now reexpress in Eq. (A1) the coupling  $a(Q^2)_{N_f=4}$  with our used  $a(Q^2)$  ( $\equiv a(Q^2)_{N_f=3}$ ) (cf. e.g., [59])

$$a(Q^2)_{N_f=4} = a(Q^2) + \frac{1}{6} \ln \left( \frac{Q^2}{m_c^2} \right) a(Q^2)^2 + \mathcal{O}(a^3), \quad (\text{A5})$$

and this leads to the expression (7) for the correction  $\delta d(Q^2)_{m_c}$  that should be interpreted as the correction due to nondecoupling of charm quark (i.e., due to  $m_c \neq \infty$ ). We note that  $d_1$  in our expansion (3) is for  $d(N_f)$  of Eq. (A4) for  $N_f = 3$ .

### Appendix B: Relations between the $\tilde{d}_n$ and $d_k$ coefficients

These relations can be obtained by first expressing the logarithmic derivatives  $\tilde{a}_n(\mu^2) \equiv \tilde{a}_n$ , Eq. (11), with the powers  $a^k \equiv a(\mu^2)^k$ . The latter relations are direct consequences of the RGE (12b) and have the form

$$\tilde{a}_n(Q^2) = a(Q^2)^n + \sum_{m=1}^{\infty} k_m(n) a(Q^2)^{n+m}. \quad (\text{B1})$$

where the coefficients  $k_m(n)$  depend only on the RGE coefficients  $c_j \equiv \beta_j/\beta_0$  and are independent of the scale  $\mu^2$  ( $= \kappa Q^2$ ). Explicit form of these relations, up to  $n = 5$ , is (note:  $\tilde{a}_1 = a$ )

$$\tilde{a}_2 = a^2 + c_1 a^3 + c_2 a^4 + c_3 a^5 + \dots, \quad (\text{B2a})$$

$$\tilde{a}_3 = a^3 + \frac{5}{2} c_1 a^4 + \left( +3c_2 + \frac{3}{2} c_1^2 \right) a^5 + \dots, \quad (\text{B2b})$$

$$\tilde{a}_4 = a^4 + \frac{13}{3} c_1 a^5 + \dots, \quad (\text{B2c})$$

$$\tilde{a}_5 = a^5 + \dots, \quad \text{etc.} \quad (\text{B2d})$$

We can invert these relations, proceeding step-by-step, and obtain

$$a^5 = \tilde{a}_5 + \dots, \quad (\text{B3a})$$

$$a^4 = \tilde{a}_4 - \frac{13}{3} c_1 \tilde{a}_5 + \dots, \quad (\text{B3b})$$

$$a^3 = \tilde{a}_3 - \frac{5}{2} c_1 \tilde{a}_4 + \left( -3c_2 + \frac{28}{3} c_1^2 \right) \tilde{a}_5 + \dots, \quad (\text{B3c})$$

$$a^2 = \tilde{a}_2 - c_1 \tilde{a}_3 + \left( -c_2 + \frac{5}{2} c_1^2 \right) \tilde{a}_4 + \left( -c_3 a^5 + \frac{22}{3} c_1 c_2 - \frac{28}{3} c_1^3 \right) \tilde{a}_5 + \dots \quad (\text{B3d})$$

When we substitute these expressions in the power expansion (8) of  $d(Q^2)$ , we obtain the reorganised series (13) in  $\tilde{a}_n$ 's with the coefficients  $\tilde{d}_n$  expressed by the original coefficients  $d_k$  ( $k = n, n-1, \dots$ )

$$\tilde{d}_0 = d_0 (= 1), \quad \tilde{d}_1 = d_1, \quad \tilde{d}_2 = d_2 - c_1 d_1, \quad (\text{B4a})$$

$$\tilde{d}_3 = d_3 - \frac{5}{2} c_1 d_2 + \left( -c_2 + \frac{5}{2} c_1^2 \right) d_1, \quad (\text{B4b})$$

$$\tilde{d}_4 = d_4 - \frac{13}{3} c_1 d_3 + \left( -3c_2 + \frac{28}{3} c_1^2 \right) d_2 + \left( -c_3 + \frac{22}{3} c_1 c_2 - \frac{28}{3} c_1^3 \right) d_1, \quad \text{etc.} \quad (\text{B4c})$$

The inverse relations can be obtained from here step-by-step, and are of the similarly linear form

$$d_n = \sum_{s=0}^{n-1} k_s(n+1-s) \tilde{d}_{n-s} \quad (n = 1, 2, \dots; k_0(m) = 1), \quad (\text{B5})$$

where the coefficients  $k_s(n+1-s)$  appearing here are those appearing also in the relations (B1). More explicitly, for  $n = 0, \dots, 4$ , these relations have the form

$$d_0 = \tilde{d}_0 (= 1), \quad d_1 = \tilde{d}_1, \quad d_2 = \tilde{d}_2 + c_1 \tilde{d}_1, \quad (\text{B6a})$$

$$d_3 = \tilde{d}_3 + \frac{5}{2} c_1 \tilde{d}_2 + c_2 \tilde{d}_1, \quad (\text{B6b})$$

$$d_4 = \tilde{d}_4 + \frac{13}{3} c_1 \tilde{d}_3 + \left( +3c_2 + \frac{3}{2} c_1^2 \right) \tilde{d}_2 + c_3 \tilde{d}_1, \quad \text{etc.} \quad (\text{B6c})$$

### Appendix C: Proof of relations Eqs. (15)

In order to prove the relations Eqs. (15), we first note that  $d \ln \mu^2 = d \ln \kappa$  (where  $\kappa \equiv \mu^2/Q^2$ ). According to the definition of the logarithmic derivatives  $\tilde{a}_n$ , Eq. (11), we have very simple recursive relations for them

$$\frac{d}{d \ln \kappa} \tilde{a}_n(\kappa Q^2) = (-\beta_0) n \tilde{a}_{n+1}(\kappa Q^2). \quad (\text{C1})$$

As a consequence, application of  $d/d \ln \kappa$  to the series Eq. (13) of  $d(Q^2)$  then gives

$$\frac{d}{d \ln \kappa} d(Q^2) = \sum_{n=1}^{\infty} \tilde{a}_{n+1}(\kappa Q^2) \left[ (-\beta_0) n \tilde{d}_{n-1}(\kappa) + \frac{d}{d \ln \kappa} \tilde{d}_n(\kappa) \right]. \quad (\text{C2})$$

However,  $d(Q^2)$  is  $\mu^2$ -independent (i.e.,  $\kappa$ -independent), therefore the above expression Eq. (C2) is identically equal to zero, hence each coefficient at  $\tilde{a}_{n+1}(\kappa Q^2)$  must be zero, and we obtain the relations Eq. (15a).

We can now apply the derivative  $d/d \ln \kappa$  to the series (14) for  $\mathcal{B}[\tilde{d}](u; \kappa)$ , take into account the (just proven) relations Eq. (15a), and we obtain

$$\frac{d}{d \ln \kappa} \mathcal{B}[\tilde{d}](u; \kappa) = u \mathcal{B}[\tilde{d}](u; \kappa), \quad (\text{C3})$$

From here, the relation (15b) follows immediately.

#### Appendix D: Renormalisation scheme dependence of the expansion coefficients

The renormalisation scheme dependence (briefly: scheme) of the coupling  $a(\mu^2; c_2, \dots)$  and of the coefficients  $d_n(\kappa; c_2, \dots)$  and  $\tilde{d}_n(\kappa; c_2, \dots)$  is the dependence on the beta-coefficients  $c_j \equiv \beta_j/\beta_0$  ( $j = 2, 3, \dots$ ) appearing in the RGE Eq. (12). The scheme of the running coupling  $a(\mu^2; c_2, c_3, \dots) \equiv a$  is governed by the following relations (cf. App. A of [24], and App. A of [39]):

$$\frac{\partial a}{\partial c_2} = a^3 + \frac{c_2}{3} a^5 + \mathcal{O}(a^6), \quad (\text{D1a})$$

$$\frac{\partial a}{\partial c_3} = \frac{1}{2} a^4 - \frac{c_1}{6} a^5 + \mathcal{O}(a^6), \quad (\text{D1b})$$

$$\frac{\partial a}{\partial c_4} = \frac{1}{3} a^5 + \mathcal{O}(a^6). \quad (\text{D1c})$$

When these relations are used in the power expansion Eq. (8) of the canonical ( $D = 0$ ) BSR  $d(Q^2)$ , and we take into account that  $d(Q^2)$  is scheme-independent (i.e., independent of  $c_2, c_3, c_4, \dots$ ), we obtain the explicit scheme-dependence of the expansion coefficients  $d_n = d_n(\kappa; c_2, c_3, \dots)$  (note:  $\kappa = \mu^2/Q^2$  is considered fixed here)

$$d_1(\kappa) = \bar{d}_1(\kappa), \quad d_2(\kappa; c_2) = \bar{d}_2(\kappa) - (c_2 - \bar{c}_2), \quad (\text{D2a})$$

$$d_3(\kappa; c_2, c_3) = \bar{d}_3(\kappa) - 2(c_2 - \bar{c}_2)\bar{d}_1(\kappa) - \frac{1}{2}(c_3 - \bar{c}_3), \quad (\text{D2b})$$

$$d_4(\kappa; c_2, c_3, c_4) = \bar{d}_4(\kappa) - 3(c_2 - \bar{c}_2)\bar{d}_2(\kappa) - (c_3 - \bar{c}_3)\bar{d}_1(\kappa) - \frac{1}{3}c_2(c_2 - \bar{c}_2) + \frac{5}{3}(c_2 - \bar{c}_2)^2 + \frac{1}{6}c_1(c_3 - \bar{c}_3) - \frac{1}{3}(c_4 - \bar{c}_4). \quad (\text{D2c})$$

Here we denoted, for simplicity:  $d_n(\kappa; \bar{c}_2, \dots, \bar{c}_n) \equiv \bar{d}_n(\kappa)$ . The scheme-dependence of the coefficients  $\tilde{d}_n(\kappa) = \tilde{d}_n(\kappa; c_2, \dots, c_n)$  is then be obtained from here, by using the relations (B4) of  $\tilde{d}_n(\kappa; c_2, \dots, c_n)$  in terms of  $d_k(\kappa; c_2, \dots, c_k)$  and for the latter we use Eqs. (D2). This gives

$$\tilde{d}_1(\kappa) = \bar{d}_1(\kappa), \quad \tilde{d}_2(\kappa; c_2) = \bar{d}_2(\kappa) - (c_2 - \bar{c}_2), \quad (\text{D3a})$$

$$\tilde{d}_3(\kappa; c_2, c_3) = \bar{d}_3(\kappa) - 2(c_2 - \bar{c}_2)\bar{d}_1(\kappa) + \frac{5}{2}c_1(c_2 - \bar{c}_2) - \frac{1}{2}(c_3 - \bar{c}_3), \quad (\text{D3b})$$

$$\begin{aligned} \tilde{d}_4(\kappa; c_2, c_3, c_4) = & \bar{d}_4(\kappa) - 3(c_2 - \bar{c}_2)\bar{d}_2(\kappa) + \left[ +\frac{17}{3}c_1(c_2 - \bar{c}_2) - (c_3 - \bar{c}_3) \right] \bar{d}_1(\kappa) \\ & + \left[ \left( -\frac{28}{3}c_1^2 + \frac{8}{3}c_2 \right) (c_2 - \bar{c}_2) + \frac{5}{3}(c_2 - \bar{c}_2)^2 + \frac{7}{3}c_1(c_3 - \bar{c}_3) - \frac{1}{3}(c_4 - \bar{c}_4) \right], \end{aligned} \quad (\text{D3c})$$

where we denoted, for simplicity:  $\tilde{d}_n(\kappa; \bar{c}_2, \dots, \bar{c}_n) \equiv \bar{d}_n(\kappa)$ .

#### Appendix E: The experimental uncorrelated uncertainty of the extracted parameter values

We summarise here the formula for the uncorrelated experimental uncertainties for the two-parameter fit ( $\bar{f}_2$  and  $\mu_6$ ) of the (inelastic) BSR. This is a special case of the approach given in App. of Ref. [53] (and App. D of [29]).<sup>15</sup>

---

<sup>15</sup> The latter approach is valid even in the case when we have known nonzero correlations of experimental data.

The fit consist of minimising the expression  $\chi^2$  Eq. (42), where the two OPE parameters  $p_1 = \bar{f}_2$  and  $p_2 = \mu_6$  are varied. The corresponding variations of these two parameters, due to the experimental uncertainties  $\sigma(Q_j^2)$  at each point  $Q_j^2$ , are

$$\begin{aligned}\langle \delta p_1 \delta p_1 \rangle &= (A^{-1})_{1,1}, \\ \langle \delta p_2 \delta p_2 \rangle &= (A^{-1})_{2,2},\end{aligned}\tag{E1a}$$

where the  $2 \times 2$  matrix  $A$  is

$$A_{\ell,m} = \sum_{j=j_{\min}}^{j_{\max}} \frac{\partial \bar{\Gamma}_1^{\text{P-n}}(Q_j^2)}{\partial p_\ell} \frac{\partial \bar{\Gamma}_1^{\text{P-n}}(Q_j^2)}{\partial p_m} \frac{1}{\sigma(Q_j^2)^2} \quad (\ell, m = 1, 2).\tag{E2}$$

Then the (uncorrelated) experimental uncertainties of the extracted values of  $p_1 = \bar{f}_2$  and of  $p_2 = \mu_6$  are

$$\delta \bar{f}_2(\text{exp.u.}) = \sqrt{\langle \delta p_1 \delta p_1 \rangle} = \sqrt{(A^{-1})_{1,1}},\tag{E3a}$$

$$\delta \mu_6(\text{exp.u.}) = \sqrt{\langle \delta p_2 \delta p_2 \rangle} = \sqrt{(A^{-1})_{2,2}},\tag{E3b}$$

In the case of the one-parameter fit ( $\bar{f}_2$ ), analogous formulas hold,  $A$  is in such a case only a number ( $1 \times 1$  matrix).

### Appendix F: $2\delta\text{AQCD}$ and $3\delta\text{AQCD}$

Here we summarise the construction of  $2\delta\text{AQCD}$  [31, 32]<sup>16</sup> and  $3\delta\text{AQCD}$  [33, 34], i.e., versions  $\mathcal{A}(Q^2)$  of the QCD coupling that have no Landau singularities and practically coincide at high  $Q^2 > 1 \text{ GeV}^2$  with the underlying pQCD coupling  $a(Q^2)$  running in a P44-renormalisation scheme, Eqs. (35)-(38). At low  $Q^2 \lesssim 1 \text{ GeV}^2$ , the coupling  $\mathcal{A}(Q^2)$  is required to fulfill certain additional conditions.

The starting point is the pQCD coupling  $a(Q^2)$  in a certain renormalisation scheme, for convenience the P44-scheme with chosen values of the scheme parameters  $c_2$  and  $c_3$ , cf. Eqs. (35)-(38). The resulting underlying ( $N_f = 3$ ) pQCD coupling  $a(Q^2)$  is given in Eq. (37), it is given in terms of the Lambert function  $W_{\pm 1}(z)$  (which is very convenient in practical evaluations), and it is an explicit function of any complex  $Q^2$ . This coupling  $a(Q^2)$  has discontinuity (cut) along the real axis; this discontinuity is usually called the spectral function of the coupling

$$\rho^{(\text{pt})}(\sigma) \equiv \text{Im } a(-\sigma - i\epsilon),\tag{F1}$$

which is thus again written in terms of the Lambert function  $W_{\pm 1}(z)$  (and thus easily evaluated in practice). Since the coupling has Landau singularities, the spectral function is nonzero not just for  $\sigma > 0$  (i.e.,  $Q^2 = -\sigma < 0$ ), but also at some lower negative values  $-\Lambda^2 \leq \sigma \leq 0$  (i.e.,  $0 \leq Q^2 = -\sigma \leq \Lambda^2$ ) where usually  $\Lambda^2 \sim 0.1 \text{ GeV}^2$ .

The holomorphic coupling  $\mathcal{A}(Q^2)$  is then required to have the spectral function  $\rho_{\mathcal{A}}(\sigma) \equiv \text{Im } \mathcal{A}(-\sigma - i\epsilon)$  which coincides with the above spectral function  $\rho^{(\text{pt})}(\sigma)$  for sufficiently large  $\sigma > M_0^2$  ( $> 0$ ); for  $0 < \sigma < M_0^2$  deviations from  $\rho^{(\text{pt})}(\sigma)$  are expected; and for  $\sigma < 0$  we require that  $\rho_{\mathcal{A}}(\sigma) = 0$  (i.e., that there are no Landau singularities). In the range  $0 < \sigma < M_0^2$  where  $\rho_{\mathcal{A}}(\sigma)$  is not known, we parametrise it by a linear combination of  $n$  Dirac delta functions [which corresponds to near-diagonal Padé expression contribution in  $\mathcal{A}(Q^2)$ , see later]

$$\rho_{\mathcal{A}}^{(n\delta)}(\sigma) = \pi \sum_{j=1}^n \mathcal{F}_j \delta(\sigma - M_j^2) + \Theta(\sigma - M_0^2) \rho^{(\text{pt})}(\sigma).\tag{F2}$$

By notational convention, we have  $(0 <) M_1^2 < M_2^2 < \dots < M_n^2 < M_0^2$ , and  $M_1^2 = M_{\text{thr}}^2$  is interpreted as the threshold scale of the spectral function  $\rho_{\mathcal{A}}$ ; it is expected to be in the range of the lowest hadronic scales, i.e.,  $M_1^2 \sim m_\pi^2$

<sup>16</sup> In [31, 32], we constructed  $2\delta\text{AQCD}$  in a class of renormalisation schemes where only  $c_2$  scheme parameter is adjustable (“3-loop” adjustable), while here we present  $2\delta\text{AQCD}$  in the P44-class of renormalisation schemes, Eqs. (35)-(38), which have  $c_2$  and  $c_3$  scheme parameters adjustable (“4-loop” adjustable).

TABLE III: Values of the parameters of the  $2\delta\text{AQCD}$  coupling used in this work; the first entry is for the central case: P44-scheme with  $c_2 = 9.$  and  $c_3 = 20.$ ;  $M_1 = 0.150$  GeV;  $\alpha_s^{\overline{\text{MS}}}(M_Z^2) = 0.1179$ ; the other entries are for the case when one of these parameters changes. The dimensionless parameters are  $s_j = M_j^2/\Lambda_L^2$  and  $f_j = \mathcal{F}_j/\Lambda_L^2$ .  $\Lambda_L$  is the Lambert scale of the underlying pQCD coupling, fixed by the condition  $\alpha_s^{\overline{\text{MS}}}(M_Z^2) = 0.1179$ .

case	$s_1$	$s_2$	$f_1$	$f_2$	$s_0$	$\Lambda_L$ [GeV]
central	0.47584	68.8281	1.71541	0.94206	95.8788	0.21745
$c_2 = 11., c_3 = 20.$	0.47581	80.6865	1.93086	1.07273	112.47	0.21745
$c_2 = 7.6, c_3 = 20.$	0.47583	61.3845	1.57632	0.85810	85.4648	0.21745
$c_2 = 9., c_3 = 35.$	0.77003	121.627	2.92848	1.62931	169.534	0.17094
$c_2 = 9., c_3 = 5.$	0.22581	28.9299	0.75915	0.40791	40.2527	0.31566
$M_1 = 0.250$ GeV	1.32175	74.2430	1.77216	0.98111	103.039	0.21745
$M_1 = 0.100$ GeV	0.21148	67.1287	1.69729	0.92969	93.6321	0.21745
$\alpha_s^{\overline{\text{MS}}}(M_Z^2) = 0.1188$	0.43937	68.5939	1.71292	0.94036	95.5691	0.22630
$\alpha_s^{\overline{\text{MS}}}(M_Z^2) = 0.1170$	0.51606	69.0864	1.7181	0.94393	96.2202	0.20881

TABLE IV: Values of the parameters of the  $3\delta\text{AQCD}$  coupling used in this work; the first entry is for the central case: P44 LMM scheme (i.e.,  $c_2 = 9.29703$  and  $c_3 = 71.4538$ );  $M_1 = 0.150$  GeV;  $\alpha_s^{\overline{\text{MS}}}(M_Z^2) = 0.1179$ ; the other entries are for the case when  $M_1$  changes, or  $\alpha_s^{\overline{\text{MS}}}(M_Z^2)$  changes. The dimensionless parameters are  $s_j = M_j^2/\Lambda_L^2$  and  $f_j = \mathcal{F}_j/\Lambda_L^2$ .  $\Lambda_L$  is the Lambert scale of the underlying pQCD coupling.

case	$s_1$	$s_2$	$s_3$	$f_1$	$f_2$	$f_3$	$s_0$	$\Lambda_L$ [GeV]
central	1.79371	42.9853	607.164	-0.586232	10.6669	6.06743	827.469	0.11200
$M_1 = 0.250$ GeV	4.98252	16.7070	470.372	-4.37049	13.2756	5.23222	647.009	0.11200
$M_1 = 0.100$ GeV	0.79720	88.0403	862.126	-0.16976	12.2415	7.52131	1163.66	0.11200
$\alpha_s^{\overline{\text{MS}}}(M_Z^2) = 0.1188$	1.65625	40.3300	589.951	-0.562248	10.5011	5.9629	804.698	0.11655
$\alpha_s^{\overline{\text{MS}}}(M_Z^2) = 0.1170$	1.94533	45.8556	625.783	-0.61228	10.8448	6.17983	852.102	0.10755

( $\sim 10^{-2}$  GeV<sup>2</sup>). On the other hand,  $M_0^2$  ( $\sim 1$  GeV<sup>2</sup>) can be interpreted as the pQCD-onset scale. Using the Cauchy theorem, we then obtain from the spectral function (F2) the running coupling  $\mathcal{A}(Q^2)$

$$\mathcal{A}^{(n\delta)}(Q^2) \left( \equiv \frac{1}{\pi} \int_0^\infty d\sigma \frac{\rho_{\mathcal{A}}(\sigma)}{(\sigma + Q^2)} \right) = \sum_{j=1}^n \frac{\mathcal{F}_j}{(Q^2 + M_j^2)} + \frac{1}{\pi} \int_{M_0^2}^\infty d\sigma \frac{\rho_1^{(\text{pt})}(\sigma)}{(Q^2 + \sigma)}. \quad (\text{F3})$$

The obtained coupling has altogether  $(2n + 1)$  parameters:  $\mathcal{F}_j$  and  $M_j^2$  ( $j = 1, \dots, n$ ) and  $M_0^2$ .<sup>17</sup> They are then fixed by various conditions. The condition that the coupling should practically coincide with the underlying pQCD coupling  $a(Q^2)$  at sufficiently high  $|Q^2| > 1$  GeV<sup>2</sup> is implemented in our approach in the following specific way:

$$\mathcal{A}(Q^2) - a(Q^2) \sim \left( \frac{\Lambda_L^2}{Q^2} \right)^5 \quad (|Q^2| > \Lambda_L^2). \quad (\text{F4})$$

In general, the above difference would<sup>18</sup> be  $\sim (\Lambda_L^2/Q^2)^1$ ; therefore, the condition (F4) represents four conditions.

In the  $2\delta\text{AQCD}$ , we have  $n = 2$  and thus five parameters. We can choose a value of the threshold scale  $M_1^2$  as an input, and then the four remaining parameters are fixed by the conditions (F4). We note that in the  $2\delta\text{AQCD}$ , the underlying pQCD coupling can be in any chosen P44-scheme (i.e., with any chosen values of  $c_2$  and  $c_3$ ).

In  $3\delta\text{AQCD}$ , we have  $n = 3$  and thus seven parameters. The conditions (F4) represent four conditions. Two additional conditions are obtained if we require that  $\mathcal{A}(Q^2)^{(3\delta)}$  behaves at low  $Q^2$  as a specific product of the Landau gauge gluon and ghost dressing functions whose behaviour at low positive  $Q^2$  was obtained by large volume lattice

<sup>17</sup> We note that we have the Lambert scale  $\Lambda_L$  in the underlying pQCD coupling, Eq. (38), and thus in  $\rho^{(\text{pt})}(\sigma)$ , but this scale is fixed by the chosen value of  $\alpha_s^{\overline{\text{MS}}}(M_Z^2)$ , as explained in Sec. V.

<sup>18</sup> The difference (F4) is  $\sim (\Lambda_L^2/Q^2)^1$  in, e.g., Minimal Analytic framework (MA; named also (F)APT) [60–64], i.e., the QCD variant in which the spectral function of the coupling is [instead of Eq. (F2)]:  $\rho_{\mathcal{A}}^{(\text{MA})}(\sigma) = \Theta(\sigma)\rho^{(\text{pt})}(\sigma)$ .

calculations [54, 55]. For details we refer to [33, 34]. These two conditions,<sup>19</sup> are that  $\mathcal{A}(Q^2)$  at positive  $Q^2$  achieves the local maximum at  $Q^2 \approx 0.135 \text{ GeV}^2$  and that it behaves as  $\mathcal{A}(Q^2) \sim Q^2$  ( $\rightarrow 0$ ) at very low  $Q^2$  ( $0 < Q^2 \lesssim 0.1 \text{ GeV}^2$ ). This gives us additional two conditions, adding up to altogether six conditions. The seventh condition, necessary to fix all the seven parameters, is again the choice of the threshold scale  $M_1^2$  ( $\sim m_\pi^2$ ).

In Tables III and IV we present the values of the parameters of the  $2\delta\text{AQCD}$  and  $3\delta\text{AQCD}$  coupling for the relevant cases used in this work.<sup>20</sup>

In Fig. 8 we present the behaviour of various ( $N_f = 3$ ) running couplings: pQCD coupling  $a(Q^2)_{\overline{\text{MS}}}$  in the 5-loop  $\overline{\text{MS}}$  scheme; pQCD coupling  $a(Q^2)$  in the P44-scheme with  $c_2 = 9.$  and  $c_3 = 20.$ ;  $2\delta\text{AQCD}$  coupling  $\mathcal{A}(Q^2)^{(2\delta)}$  (in the mentioned P44 scheme with  $c_2 = 9.$  and  $c_3 = 20.$ ); and  $3\delta\text{AQCD}$  coupling  $\mathcal{A}(Q^2)^{(3\delta)}$  in the P44 LMM scheme ( $c_2 = 9.29703$  and  $c_3 = 71.4538$ ). The coupling  $a(Q^2)$  has Landau cut for  $Q^2 < 0.87 \text{ GeV}^2$ , and  $a(Q^2)_{\overline{\text{MS}}}$

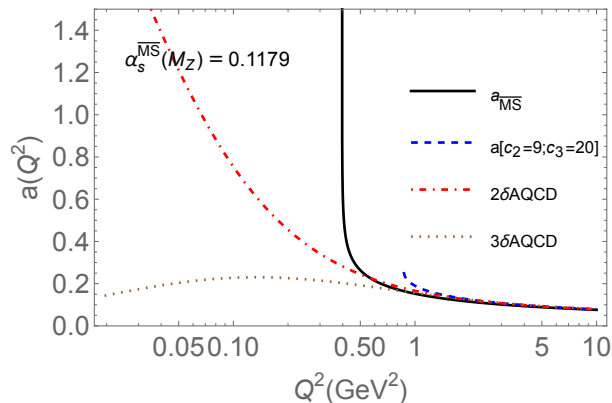


FIG. 8: Various ( $N_f = 3$ ) running couplings: pQCD coupling  $a(Q^2)_{\overline{\text{MS}}}$  in the 5-loop  $\overline{\text{MS}}$  scheme;  $2\delta\text{AQCD}$  coupling  $\mathcal{A}(Q^2)^{(2\delta)}$  and its underlying pQCD coupling  $a(Q^2)$ , both in the P44 scheme with  $c_2 = 9.$  and  $c_3 = 20.$ ;  $3\delta\text{AQCD}$  coupling  $\mathcal{A}(Q^2)^{(3\delta)}$ , in the (lattice-related) P44 LMM scheme.

for  $Q^2 < 0.40 \text{ GeV}^2$ . We note that at the corresponding branching points  $a(Q^2)$  is finite and  $a(Q^2)_{\overline{\text{MS}}}$  is infinite. The AQCD couplings have neither Landau cuts nor infinities. The coupling  $\mathcal{A}(Q^2)^{(2\delta)}$  grows at decreasing  $Q^2$  and reaches a large, but finite value  $\mathcal{A}(0)^{(2\delta)} = 3.6970$  at  $Q^2 = 0$ . All couplings correspond to the reference value  $\alpha_s^{\overline{\text{MS}}}(M_Z^2; N_f = 5) = 0.1179$ , and the AQCD couplings have the spectral threshold scale  $M_1 = 0.150 \text{ GeV}$ .

Further, in Figs. 9(a),(b), we present separately the  $2\delta\text{AQCD}$  and  $3\delta\text{AQCD}$  running couplings; for comparison, we include the corresponding underlying pQCD couplings  $a(Q^2)$ .

<sup>19</sup> These two conditions are in the (lattice-related)  $N_f = 3$  MiniMOM scheme (MM) [42–45] ( $c_2^{\text{MM}} = 9.29703$ ;  $c_3^{\text{MM}} = 71.4538$ ) with  $\overline{\text{MS}}$  scaling convention (LMM, i.e., Lambert MiniMOM).

<sup>20</sup> We note in Table III that, when  $c_2$  changes and  $c_3$  is kept fixed in P44 scheme,  $\Lambda_L$  changes very little,  $\delta\Lambda_L \lesssim 10^{-6}$ .

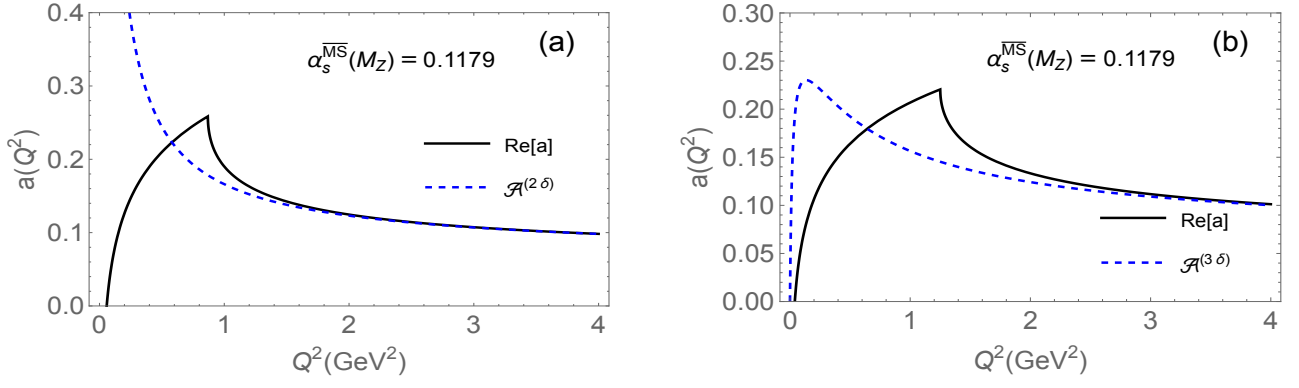


FIG. 9: The AQCD running coupling  $\mathcal{A}(Q^2)$  and their corresponding underlying pQCD coupling  $a(Q^2)$ : (a) for  $2\delta$ AQCD (in the scheme P44 with  $c_2 = 9$ , and  $c_3 = 20$ .); (b) for  $3\delta$ AQCD (in the P44 LMM scheme). The coupling  $a(Q^2)$  has Landau cut at  $0 \leq Q^2 < 0.87 \text{ GeV}^2$  in the  $2\delta$  case, and at  $0 \leq Q^2 < 1.25 \text{ GeV}^2$  in the  $3\delta$  case. Both these couplings  $a(Q^2)$  become complex on the Landau cut. Therefore, real part  $\text{Re } a(Q^2)$  was presented in those intervals.

The expansions in AQCD are made in a completely analogous way as in Eq. (13) in pQCD, i.e., in terms of the logarithmic derivatives  $\tilde{\mathcal{A}}_2$  which are the AQCD analogs of the  $\tilde{a}_n$  logarithmic derivatives of Eq. (11)

$$\tilde{\mathcal{A}}_n(\mu^2) \equiv \frac{(-1)^{n-1}}{(n-1)! \beta_0^{n-1}} \left( \frac{d}{d \ln \mu^2} \right)^{n-1} \mathcal{A}(\mu^2) \quad (n = 1, 2, \dots). \quad (\text{F5})$$

The expansion in AQCD has the form analogous to Eq. (13) [65]<sup>21,22</sup>

$$d(Q^2) = \mathcal{A}(\kappa Q^2) + \tilde{d}_1(\kappa) \tilde{\mathcal{A}}_2(\kappa Q^2) + \dots + \tilde{d}_n(\kappa) \tilde{\mathcal{A}}_{n+1}(\kappa Q^2) + \dots, \quad (\text{F6})$$

Another, more efficient, sequence of approximants are specific type of approximants,  $\mathcal{G}_d^{[M/M]}(Q^2)$ , which are related to the diagonal Padé approximants, and are constructed only on the basis of the knowledge of the first  $2M$  coefficients of the series (13), or equivalently of the series (F6):  $\tilde{d}_j(\kappa)$  ( $j = 0, 1, \dots, 2M - 1$ ). The approximants  $\mathcal{G}_d^{[M/M]}(Q^2)$  were proposed in [46] in the context of pQCD, and were later applied in variants of AQCD in [23, 47–49] to the (spacelike) Adler function and to related QCD observables. They are completely independent of the renormalisation scale parameter  $\kappa$ .<sup>23</sup> These approximants have in AQCD the form

$$\mathcal{G}_d^{[M/M]}(Q^2)_{\text{AQCD}} = \sum_{k=1}^M \tilde{\alpha}_j \mathcal{A}(\kappa_j Q^2), \quad (\text{F7})$$

and fulfill the approximant precision relation

$$d(Q^2) - \mathcal{G}_d^{[M/M]}(Q^2)_{\text{AQCD}} = \mathcal{O}(\tilde{\mathcal{A}}_{2M+1}) = \mathcal{O}(a^{2M+1}). \quad (\text{F8})$$

In pQCD, the same expression (F7) is valid, but with  $\mathcal{A}(\kappa_j Q^2)$  replaced by the pQCD coupling  $a(\kappa_j Q^2)$ .

We note that the approximant (F7) contains in total  $2M$  parameters:  $\tilde{\alpha}_j$  and  $\kappa_j$ , which are determined by the first  $2M$  expansion coefficients  $\tilde{d}_n(\kappa)$  ( $n = 0, 1, \dots, 2M - 1$ ).<sup>24</sup> As noted in [46], the application of these approximants in pQCD gives for spacelike QCD observables  $d(Q^2)$  in general relatively unstable results, especially when  $M$  increases, and this is so because some of the  $\kappa_j$  coefficients are very small and then  $a(\kappa_j Q^2)$  is on Landau cut singularities. This problem does not appear in QCD with holomorphic couplings (AQCD), as noted in [23, 47–49], because  $\mathcal{A}(\kappa_j Q^2)$  coupling has no Landau singularities.

<sup>21</sup> The extension of the logarithmic derivative,  $\tilde{\mathcal{A}}_\nu(Q^2)$ , for noninteger  $\nu$  in any AQCD was constructed in [66], as well as the coupling  $\mathcal{A}_\nu(Q^2)$  that is the AQCD analog of the power  $a(Q^2)^\nu$  (for  $\nu$  noninteger,  $-1 < \nu$ ). For the Minimal Analytic (MA) QCD, the extended logarithmic derivatives  $\tilde{\mathcal{A}}_\nu^{(\text{MA})}(Q^2)$  were constructed as explicit functions at one-loop order in [63] and at any loop order in [67].

<sup>22</sup> For some applications of various AQCD to QCD phenomenology, see, e.g., [15, 66, 68–77].

<sup>23</sup> The corresponding diagonal Padé approximants are  $\kappa$ -invariant only at the one-loop level approximation [78].

<sup>24</sup> We note that  $\tilde{d}_0 = 1$ , and therefore  $\sum \tilde{\alpha}_j = 1$ .



TABLE V: Values of the parameters  $\tilde{\alpha}_j$  and  $\kappa_j$  of the (diagonal Padé-related) approximants  $\mathcal{G}_d^{[M/M]}(Q^2)$ , for  $2\delta\text{AQCD}$  and  $3\delta\text{AQCD}$  (in their respective P44-schemes), for  $M = 2$  and  $M = 3$ .

QCD variant	$M$	$\tilde{\alpha}_1$	$\tilde{\alpha}_2$	$\tilde{\alpha}_3$	$\kappa_1$	$\kappa_2$	$\kappa_3$
$2\delta\text{AQCD}$	2	-0.011789	1.011789	–	462.707872	0.222567	–
$2\delta\text{AQCD}$	3	-0.045853	0.013012	1.032841	20.911126	0.0033448	0.263115
$3\delta\text{AQCD}$	2	-0.044854	1.044854	–	13.47291	0.243514	–
$3\delta\text{AQCD}$	3	-0.095297	0.008018	1.087279	4.781674	0.006406	0.275173

In Table V we present the values of the parameters  $\kappa_j$  and  $\tilde{\alpha}_j$  of the approximants  $\mathcal{G}_d^{[M/M]}(Q^2)$  for canonical BSR  $d(Q^2)$ , for  $M = 2$  and  $M = 3$ , for  $2\delta\text{QCD}$  (in the P44 scheme with  $c_2 = 9$ . and  $c_3 = 20$ .) and for  $3\delta\text{AQCD}$  (in the P44 LMM scheme, i.e., with  $c_2 = 9.29703$  and  $c_3 = 71.4538$ ).

- 
- [1] J. D. Bjorken, “Applications of the Chiral  $U(6) \times (6)$  Algebra of Current Densities,” Phys. Rev. **148** (1966), 1467-1478
- [2] J. D. Bjorken, “Inelastic Scattering of Polarized Leptons from Polarized Nucleons,” Phys. Rev. D **1** (1970), 1376-1379
- [3] B. Adeva *et al.* [Spin Muon (SMC)], “The Spin dependent structure function  $g_1(x)$  of the proton from polarized deep inelastic muon scattering,” Phys. Lett. B **412** (1997), 414-424;
- D. Adams *et al.* [Spin Muon (SMC)], “Spin structure of the proton from polarized inclusive deep inelastic muon - proton scattering,” Phys. Rev. D **56** (1997), 5330-5358 [arXiv:hep-ex/9702005 [hep-ex]];
- E. S. Ageev *et al.* [COMPASS], “Measurement of the spin structure of the deuteron in the DIS region,” Phys. Lett. B **612** (2005), 154-164 [arXiv:hep-ex/0501073 [hep-ex]];
- V. Y. Alexakhin *et al.* [COMPASS], “The Deuteron Spin-dependent Structure Function  $g_1^d$  and its First Moment,” Phys. Lett. B **647** (2007), 8-17 [arXiv:hep-ex/0609038 [hep-ex]];
- M. G. Alekseev *et al.* [COMPASS], “The Spin-dependent Structure Function of the Proton  $g_1^p$  and a Test of the Bjorken Sum Rule,” Phys. Lett. B **690** (2010), 466-472 [arXiv:1001.4654 [hep-ex]];
- C. Adolph *et al.* [COMPASS], “The spin structure function  $g_1^p$  of the proton and a test of the Bjorken sum rule,” Phys. Lett. B **753** (2016), 18-28 [arXiv:1503.08935 [hep-ex]];
- C. Adolph *et al.* [COMPASS], “Final COMPASS results on the deuteron spin-dependent structure function  $g_1^d$  and the Bjorken sum rule,” Phys. Lett. B **769** (2017), 34-41 [arXiv:1612.00620 [hep-ex]];
- M. Aghasyan *et al.* [COMPASS], “Longitudinal double-spin asymmetry  $A_1^p$  and spin-dependent structure function  $g_1^p$  of the proton at small values of  $x$  and  $Q^2$ ,” Phys. Lett. B **781** (2018), 464-472 [arXiv:1710.01014 [hep-ex]]
- [4] K. Ackerstaff *et al.* [HERMES], “Measurement of the neutron spin structure function  $g_1^n$  with a polarized  $^3\text{He}$  internal target,” Phys. Lett. B **404** (1997), 383-389 [arXiv:hep-ex/9703005 [hep-ex]];
- A. Airapetian *et al.* [HERMES], “Measurement of the proton spin structure function  $g_1^p$  with a pure hydrogen target,” Phys. Lett. B **442** (1998), 484-492 [arXiv:hep-ex/9807015 [hep-ex]]
- [5] K. Abe *et al.* [E143], “Measurements of the proton and deuteron spin structure functions  $g_1$  and  $g_2$ ,” Phys. Rev. D **58** (1998), 112003 [arXiv:hep-ph/9802357 [hep-ph]];
- P. L. Anthony *et al.* [E142], “Deep inelastic scattering of polarized electrons by polarized  $^3\text{He}$  and the study of the neutron spin structure,” Phys. Rev. D **54** (1996), 6620-6650 [arXiv:hep-ex/9610007 [hep-ex]];
- K. Abe *et al.* [E154], “Precision determination of the neutron spin structure function  $g_1^n$ ,” Phys. Rev. Lett. **79** (1997), 26-30 [arXiv:hep-ex/9705012 [hep-ex]];
- P. L. Anthony *et al.* [E155], “Measurement of the deuteron spin structure function  $g_1^d(x)$  for  $1 \text{ (GeV/c)}^2 < Q^2 < 40 \text{ (GeV/c)}^2$ ,” Phys. Lett. B **463** (1999), 339-345 [arXiv:hep-ex/9904002 [hep-ex]];
- P. L. Anthony *et al.* [E155], “Measurements of the  $Q^2$  dependence of the proton and neutron spin structure functions  $g_1^p$  and  $g_1^n$ ,” Phys. Lett. B **493** (2000), 19-28. [arXiv:hep-ph/0007248 [hep-ph]]
- [6] A. Deur *et al.*, “Experimental determination of the evolution of the Bjorken integral at low  $Q^2$ ,” Phys. Rev. Lett. **93** (2004), 212001 [arXiv:hep-ex/0407007 [hep-ex]]
- [7] A. Deur *et al.*, “Experimental study of isovector spin sum rules,” Phys. Rev. D **78** (2008), 032001 [arXiv:0802.3198 [nucl-ex]]
- [8] K. Slifer *et al.* [Resonance Spin Structure], “Probing quark-gluon interactions with transverse polarized scattering,” Phys. Rev. Lett. **105** (2010), 101601 [arXiv:0812.0031 [nucl-ex]]
- [9] A. Deur *et al.*, “High precision determination of the  $Q^2$  evolution of the Bjorken Sum,” Phys. Rev. D **90** (2014) no.1, 012009 [arXiv:1405.7854 [nucl-ex]]
- [10] K. P. Adhikari *et al.* [CLAS], “Measurement of the  $Q^2$  dependence of the Deuteron spin structure function  $g_1$  and its moments at low  $Q^2$  with CLAS,” Phys. Rev. Lett. **120** (2018) no.6, 062501 [arXiv:1711.01974 [nucl-ex]];
- X. Zheng *et al.* [CLAS], “Measurement of the proton spin structure at long distances,” Nature Phys. **17** (2021) no.6, 736-741 [arXiv:2102.02658 [nucl-ex]];
- V. Sulkosky *et al.* [Jefferson Lab E97-110], “Measurement of the  $^3\text{He}$  spin-structure functions and of neutron ( $^3\text{He}$ ) spin-dependent sum rules at  $0.035 \leq Q^2 \leq 0.24 \text{ GeV}^2$ ,” Phys. Lett. B **805** (2020), 135428 [arXiv:1908.05709 [nucl-ex]]

- [11] S. G. Gorishnii and S. A. Larin, “QCD corrections to the parton model rules for Structure functions of Deep Inelastic Scattering,” *Phys. Lett. B* **172** (1986), 109-112
- [12] S. A. Larin and J. A. M. Vermaseren, “The  $\alpha_s^3$  corrections to the Bjorken sum rule for polarized electroproduction and to the Gross-Llewellyn Smith sum rule,” *Phys. Lett. B* **259** (1991), 345-352
- [13] P. A. Baikov, K. G. Chetyrkin and J. H. Kühn, “Adler function, Bjorken Sum Rule, and the Crewther relation to order  $\alpha_s^4$  in a general gauge theory,” *Phys. Rev. Lett.* **104** (2010), 132004 [arXiv:1001.3606 [hep-ph]]
- [14] G. Altarelli, R. D. Ball, S. Forte and G. Ridolfi, “Determination of the Bjorken sum and strong coupling from polarized structure functions,” *Nucl. Phys. B* **496** (1997), 337-357 [arXiv:hep-ph/9701289 [hep-ph]]
- [15] C. Ayala, G. Cvetič, A. V. Kotikov and B. G. Shaikhatdenov, “Bjorken polarized sum rule and infrared-safe QCD couplings,” *Eur. Phys. J. C* **78** (2018) no.12, 1002 [arXiv:1812.01030 [hep-ph]]
- [16] D. Kotlorz and S. V. Mikhailov, “Optimized determination of the polarized Bjorken sum rule in pQCD,” *Phys. Rev. D* **100** (2019) no.5, 056007 [arXiv:1810.02973 [hep-ph]]
- [17] Q. Yu, X. G. Wu, H. Zhou and X. D. Huang, “A novel determination of non-perturbative contributions to Bjorken sum rule,” *Eur. Phys. J. C* **81** (2021) no.8, 690 [arXiv:2102.12771 [hep-ph]]
- [18] C. Ayala, C. Castro-Arriaza and G. Cvetič, “Evaluation of Bjorken polarised sum rule with a renormalon-motivated approach,” *Phys. Lett. B* **848** (2024), 138386 [arXiv:2309.12539 [hep-ph]]
- [19] R. L. Workman *et al.* [Particle Data Group], “Review of Particle Physics,” *PTEP* **2022** (2022), 083C01, and 2023 update
- [20] A. L. Kataev and V. V. Starshenko, “Estimates of the higher order QCD corrections to  $R(s)$ ,  $R_\tau$  and Deep Inelastic Scattering sum rules,” *Mod. Phys. Lett. A* **10** (1995), 235-250 [arXiv:hep-ph/9502348 [hep-ph]]
- [21] H. Kawamura, T. Uematsu, J. Kodaira and Y. Yasui, “Renormalization of twist four operators in QCD Bjorken and Ellis-Jaffe sum rules,” *Mod. Phys. Lett. A* **12** (1997), 135-143 [arXiv:hep-ph/9603338 [hep-ph]]
- [22] J. Blümlein, G. Falcioni and A. De Freitas, “The complete  $O(\alpha_s^3)$  non-singlet heavy flavor corrections to the structure functions  $g_{1,2}^{ep}(x, Q^2)$ ,  $F_{1,2,L}^{ep}(x, Q^2)$ ,  $F_{1,2,3}^{\nu(\bar{\nu})}(x, Q^2)$  and the associated sum rules,” *Nucl. Phys. B* **910** (2016) 568 [arXiv:1605.05541 [hep-ph]]
- [23] G. Cvetič, “Renormalon-motivated evaluation of QCD observables,” *Phys. Rev. D* **99** (2019) no.1, 014028 [arXiv:1812.01580 [hep-ph]]
- [24] P. M. Stevenson, “Optimized Perturbation Theory,” *Phys. Rev. D* **23** (1981), 2916
- [25] D. J. Broadhurst and A. L. Kataev, “Connections between deep inelastic and annihilation processes at next to next-to-leading order and beyond,” *Phys. Lett. B* **315** (1993), 179-187 [arXiv:hep-ph/9308274 [hep-ph]]
- [26] M. Beneke, “Renormalons,” *Phys. Rept.* **317** (1999), 1-142 [arXiv:hep-ph/9807443 [hep-ph]]
- [27] A. L. Kataev, “Infrared renormalons and the relations between the Gross-Llewellyn Smith and the Bjorken polarized and unpolarized sum rules,” *JETP Lett.* **81** (2005), 608-611 [arXiv:hep-ph/0505108 [hep-ph]]
- [28] A. L. Kataev, “Deep inelastic sum rules at the boundaries between perturbative and nonperturbative QCD,” *Mod. Phys. Lett. A* **20** (2005), 2007-2022 [arXiv:hep-ph/0505230 [hep-ph]]
- [29] C. Ayala, G. Cvetič and D. Teca, “Borel–Laplace sum rules with  $\tau$  decay data, using OPE with improved anomalous dimensions,” *J. Phys. G* **50** (2023) no.4, 045004 [arXiv:2206.05631 [hep-ph]]
- [30] C. Castro-Arriaza, Master Thesis (in preparation).
- [31] C. Ayala, C. Contreras and G. Cvetič, “Extended analytic QCD model with perturbative QCD behavior at high momenta,” *Phys. Rev. D* **85** (2012) 114043 [arXiv:1203.6897 [hep-ph]]; in Eqs. (21) and (22) of this reference there is a typo: the lower limit of integration is written as  $s_L - \eta$ ; it is in fact  $-s_L - \eta$
- [32] C. Ayala and G. Cvetič, “anQCD: a Mathematica package for calculations in general analytic QCD models,” *Comput. Phys. Commun.* **190** (2015), 182-199 [arXiv:1408.6868 [hep-ph]]
- [33] C. Ayala, G. Cvetič, R. Kögerler and I. Kondrashuk, “Nearly perturbative lattice-motivated QCD coupling with zero IR limit,” *J. Phys. G* **45** (2018) no.3, 035001 [arXiv:1703.01321 [hep-ph]]
- [34] G. Cvetič and R. Kögerler, “Lattice-motivated QCD coupling and hadronic contribution to muon  $g - 2$ ,” *J. Phys. G* **48** (2021) no.5, 055008 [arXiv:2009.13742 [hep-ph]]
- [35] G. Cvetič and I. Kondrashuk, “Explicit solutions for effective four- and five-loop QCD running coupling,” *JHEP* **12** (2011), 019 [arXiv:1110.2545 [hep-ph]]
- [36] P. A. Baikov, K. G. Chetyrkin and J. H. Kühn, “Five-loop running of the QCD coupling constant,” *Phys. Rev. Lett.* **118** (2017) no. 8, 082002 [arXiv:1606.08659 [hep-ph]]
- [37] Y. Schröder and M. Steinhauser, “Four-loop decoupling relations for the strong coupling,” *JHEP* **0601** (2006), 051 [hep-ph/0512058]
- [38] B. A. Kniehl, A. V. Kotikov, A. I. Onishchenko and O. L. Veretin, “Strong-coupling constant with flavor thresholds at five loops in the anti-MS scheme,” *Phys. Rev. Lett.* **97** (2006), 042001 [hep-ph/0607202]
- [39] G. Cvetič and R. Kögerler, “Scale and scheme independent extension of Pade approximants: Bjorken polarized sum rule as an example,” *Phys. Rev. D* **63** (2001), 056013 [hep-ph/0006098]
- [40] F. Campanario and A. Pineda, “Fit to the Bjorken, Ellis-Jaffe and Gross-Llewellyn-Smith sum rules in a renormalon based approach,” *Phys. Rev. D* **72** (2005), 056008 [arXiv:hep-ph/0508217 [hep-ph]]
- [41] C. Ayala and A. Pineda, “Bjorken sum rule with hyperasymptotic precision,” *Phys. Rev. D* **106** (2022) no.5, 056023 [arXiv:2208.07389 [hep-ph]]
- [42] L. von Smekal, K. Maltman and A. Sternbeck, “The Strong coupling and its running to four loops in a minimal MOM scheme,” *Phys. Lett. B* **681** (2009), 336 [arXiv:0903.1696 [hep-ph]]
- [43] P. Boucaud, F. De Soto, J. P. Leroy, A. Le Yaouanc, J. Micheli, O. Pene and J. Rodríguez-Quintero, “Ghost-gluon running

- coupling, power corrections and the determination of  $\Lambda(\overline{\text{MS}})$ ,” Phys. Rev. D **79** (2009), 014508 [arXiv:0811.2059 [hep-ph]]
- [44] S. Zafeiropoulos, P. Boucaud, F. De Soto, J. Rodríguez-Quintero and J. Segovia, “Strong running coupling from the gauge sector of domain wall Lattice QCD with physical quark masses,” Phys. Rev. Lett. **122** (2019) no.16, 162002 [arXiv:1902.08148 [hep-ph]]
- [45] K. G. Chetyrkin and A. Retey, “Three loop three linear vertices and four loop similar to MOM beta functions in massless QCD,” [arXiv:hep-ph/0007088 [hep-ph]]
- [46] G. Cvetič, “Renormalization scale invariant continuation of truncated QCD (QED) series: an analysis beyond large- $\beta_0$  approximation,” Nucl. Phys. B **517** (1998), 506-520 [hep-ph/9711406]; “Improvement of the method of diagonal Padé approximants for perturbative series in gauge theories,” Phys. Rev. D **57** (1998), R3209-R3213 [hep-ph/9711487]; G. Cvetič and R. Kögerler, “Towards a physical expansion in perturbative gauge theories by using improved Baker-Gammel approximants,” Nucl. Phys. B **522** (1998), 396-410 [hep-ph/9802248]
- [47] G. Cvetič and R. Kögerler, “Applying generalized Padé approximants in analytic QCD models,” Phys. Rev. D **84** (2011), 056005 [arXiv:1107.2902 [hep-ph]]
- [48] G. Cvetič and C. Villavicencio, “Operator Product Expansion with analytic QCD in tau decay physics,” Phys. Rev. D **86** (2012), 116001 [arXiv:1209.2953 [hep-ph]]
- [49] G. Cvetič, “Techniques of evaluation of QCD low-energy physical quantities with running coupling with infrared fixed point,” Phys. Rev. D **89** (2014) no.3, 036003 [arXiv:1309.1696 [hep-ph]] [in Eq.(C22b), second line, there is a typo: instead of  $(1 + 1/t)$  there should be  $\ln(1 + 1/t)$ ; the correct formula was used there, though]
- [50] A. Deur, J. P. Chen, *et al.* “Experimental study of the behavior of the Bjorken sum at very low  $Q^2$ ,” Phys. Lett. B **825** (2022), 136878 [arXiv:2107.08133 [nucl-ex]]
- [51] P. A. Zyla *et al.* [Particle Data Group], “Review of Particle Physics,” PTEP **2020** (2020) no.8, 083C01
- [52] M. Schmelling, “Averaging correlated data,” Phys. Scripta **51** (1995), 676-679
- [53] D. Boito, O. Cata, M. Golterman, M. Jamin, K. Maltman, J. Osborne and S. Peris, “A new determination of  $\alpha_s$  from hadronic  $\tau$  decays,” Phys. Rev. D **84** (2011), 113006 [arXiv:1110.1127 [hep-ph]]
- [54] I. L. Bogolubsky, E.-M. Ilgenfritz, M. Müller-Preussker and A. Sternbeck, “Lattice gluodynamics computation of Landau gauge Green’s functions in the deep infrared,” Phys. Lett. B **676** (2009), 69 [arXiv:0901.0736 [hep-lat]]
- [55] E.-M. Ilgenfritz, M. Müller-Preussker, A. Sternbeck and A. Schiller, “Gauge-variant propagators and the running coupling from lattice QCD,” hep-lat/0601027
- [56] S. J. Brodsky, G. F. de Teramond and A. Deur, “Nonperturbative QCD Coupling and its  $\beta$ -function from Light-Front Holography,” Phys. Rev. D **81** (2010), 096010 [arXiv:1002.3948 [hep-ph]]
- [57] A. Deur, J. M. Shen, X. G. Wu, S. J. Brodsky and G. F. de Teramond, “Implications of the Principle of Maximum Conformality for the QCD strong coupling,” Phys. Lett. B **773** (2017), 98 [arXiv:1705.02384 [hep-ph]]
- [58] Web page <http://www.gcvetic.usm.cl/>. The set of mathematica programs for the case of pQCD coupling are contained in the tarred file fitBSRgenP44res.tar (some of these programs are interdependent because some of them call some of the others. The central program is fitBSRgenP44res.m). The corresponding files for the analysis with  $2\delta$ ACD and  $3\delta$ AQCD coupling are contained in fitBSRgen2dP44res.tar and fitBSRgen3dP44res.tar, respectively.
- [59] K. G. Chetyrkin, B. A. Kniehl and M. Steinhauser, “Strong coupling constant with flavor thresholds at four loops in the MS scheme,” Phys. Rev. Lett. **79** (1997), 2184-2187 [arXiv:hep-ph/9706430 [hep-ph]]
- [60] D. V. Shirkov and I. L. Solovtsov, “Analytic QCD running coupling with finite IR behaviour and universal  $\bar{\alpha}_s(0)$  value,” *JINR Rapid Commun.* **2[76]** (1996), 5-10 [arXiv:hep-ph/9604363 [hep-ph]]; “Analytic model for the QCD running coupling with universal  $\alpha_s(0)$  value,” Phys. Rev. Lett. **79** (1997), 1209 [hep-ph/9704333]
- [61] K. A. Milton and I. L. Solovtsov, “Analytic perturbation theory in QCD and Schwinger’s connection between the beta function and the spectral density,” Phys. Rev. D **55** (1997), 5295-5298 [arXiv:hep-ph/9611438 [hep-ph]]
- [62] D. V. Shirkov and I. L. Solovtsov, “Ten years of the analytic perturbation theory in QCD,” Theor. Math. Phys. **150** (2007), 132 [hep-ph/0611229]
- [63] A. P. Bakulev, S. V. Mikhailov and N. G. Stefanis, “QCD analytic perturbation theory: From integer powers to any power of the running coupling,” Phys. Rev. D **72** (2005), 074014 [Phys. Rev. D **72** (2005), 119908] [hep-ph/0506311]; “Fractional Analytic Perturbation Theory in Minkowski space and application to Higgs boson decay into a b anti-b pair,” Phys. Rev. D **75** (2007), 056005 Erratum: [Phys. Rev. D **77** (2008), 079901] [hep-ph/0607040]; “Higher-order QCD perturbation theory in different schemes: From FOPT to CIPT to FAPT,” JHEP **1006** (2010), 085 [arXiv:1004.4125 [hep-ph]]
- [64] A. P. Bakulev, “Global Fractional Analytic Perturbation Theory in QCD with Selected Applications,” Phys. Part. Nucl. **40** (2009), 715 [arXiv:0805.0829 [hep-ph]] (arXiv preprint in Russian)
- [65] G. Cvetič and C. Valenzuela, “An approach for evaluation of observables in analytic versions of QCD,” J. Phys. G **32** (2006), L27 [hep-ph/0601050]; “Various versions of analytic QCD and skeleton-motivated evaluation of observables,” Phys. Rev. D **74** (2006), 114030 [erratum: Phys. Rev. D **84** (2011), 019902] [arXiv:hep-ph/0608256 [hep-ph]]
- [66] G. Cvetič and A. V. Kotikov, “Analogues of Noninteger Powers in General Analytic QCD,” J. Phys. G **39** (2012), 065005 [arXiv:1106.4275 [hep-ph]]
- [67] A. V. Kotikov and I. A. Zemlyakov, “About derivatives in analytic QCD,” Pisma Zh. Eksp. Teor. Fiz. **115** (2022) no.10, 609; “Fractional analytic QCD beyond leading order,” J. Phys. G **50** (2023) no.1, 015001 [arXiv:2203.09307 [hep-ph]]; “Fractional analytic QCD beyond leading order in the timelike region,” Phys. Rev. D **107** (2023) no.9, 094034 [arXiv:2302.12171 [hep-ph]]
- [68] D. V. Shirkov, “Analytic perturbation theory in analyzing some QCD observables,” Eur. Phys. J. C **22** (2001), 331-340 [arXiv:hep-ph/0107282 [hep-ph]]

- [69] A. V. Nesterenko, “Analytic invariant charge in QCD,” *Int. J. Mod. Phys. A* **18** (2003), 5475-5520 [hep-ph/0308288]
- [70] A. V. Nesterenko and J. Papavassiliou, “The massive analytic invariant charge in QCD,” *Phys. Rev. D* **71** (2005), 016009 [hep-ph/0410406]; “A novel integral representation for the Adler function,” *J. Phys. G* **32** (2006), 1025 [hep-ph/0511215]
- [71] A. V. Nesterenko, “Strong interactions in spacelike and timelike domains: dispersive approach,” Elsevier, Amsterdam, 2016, eBook ISBN: 9780128034484
- [72] I. R. Gabdrakhmanov, N. A. Gramotkov, A. V. Kotikov, D. A. Volkova and I. A. Zemlyakov, “Bjorken sum rule with analytic coupling at low  $Q^2$  values,” *Pisma Zh. Eksp. Teor. Fiz.* **118** (2023) no.7, 491-492 [arXiv:2307.16225 [hep-ph]]
- [73] C. Ayala and G. Cvetič, “Calculation of binding energies and masses of quarkonia in analytic QCD models,” *Phys. Rev. D* **87** (2013) no.5, 054008 [arXiv:1210.6117 [hep-ph]]
- [74] C. Ayala and S. V. Mikhailov, “How to perform a QCD analysis of DIS in analytic perturbation theory,” *Phys. Rev. D* **92** (2015) no.1, 014028 [arXiv:1503.00541 [hep-ph]]
- [75] L. Ghasemzadeh, A. Mirjalili and S. Atashbar Tehrani, “Nonsinglet polarized nucleon structure function in infrared-safe QCD,” *Phys. Rev. D* **100** (2019) no.11, 114017 [arXiv:1906.01606 [hep-ph]]; “Analytical perturbation theory and nucleon structure function in infrared region,” *Phys. Rev. D* **104** (2021) no.7, 074007 [arXiv:2109.02372 [hep-ph]]
- [76] A. V. Nesterenko, “Hadronic vacuum polarization function within dispersive approach to QCD,” *J. Phys. G* **42** (2015), 085004 [arXiv:1411.2554 [hep-ph]]
- [77] G. Cvetič and R. Kögerler, “Infrared-suppressed QCD coupling and the hadronic contribution to muon  $g-2$ ,” *J. Phys. G* **47** (2020) no.10, 10LT01 [arXiv:2007.05584 [hep-ph]]; “Lattice-motivated QCD coupling and hadronic contribution to muon  $g-2$ ,” *J. Phys. G* **48** (2021) no.5, 055008 [arXiv:2009.13742 [hep-ph]]
- [78] E. Gardi, “Why Padé approximants reduce the renormalization scale dependence in QFT?,” *Phys. Rev. D* **56** (1997), 68-79 [hep-ph/9611453]